SUPPLEMENTARY INFORMATION

ABHD10 is an *S*-depalmitoylase affecting redox homeostasis through peroxiredoxin-5

Yang Cao[1,5], Tian Qiu[1,5], Rahul S. Kathayat[1,5], Saara-Anne Azizi[2], Anneke K. Thorne[1], Daniel Ahn[1], Yuko Fukata[3], Masaki Fukata[3], Phoebe A. Rice[4], Bryan C. Dickinson[1]*

[1]Department of Chemistry, The University of Chicago, Chicago, IL 60637, USA

[2]Medical Scientist Training Program, Pritzker School of Medicine, The University of Chicago, Chicago, IL, 60637, USA

[3]Division of Membrane Physiology, Department of Molecular and Cellular Physiology, National Institute for Physiological Sciences, National Institutes of Natural Sciences, Okazaki 444-8787, Japan

[4]Department of Biochemistry and Molecular Biology, The University of Chicago, Chicago, IL 60637, USA

[5]These authors contributed equally

*Correspondence: Dickinson@uchicago.edu (B. C. D.)

Suppplementary Table 1 | Data collection and refinement statistics of crystallization.

	mouse ABHD10 (6NY9)
Data collection	
Space group	P 63 2 2
Cell dimensions	
a, *b*, *c* (Å)	99.388, 99.388, 149.597
α, β, γ (°)	90, 90, 120
Resolution (Å)	56.46 - 1.657 (1.717 - 1.657) *
R_{sym} or R_{merge}	0.1082 (2.72)
I / σI	20.82 (1.60)
Completeness (%)	92.82 (76.98)
Redundancy	12.9 (12.8)
Refinement	
Resolution (Å)	56.46 - 1.657
No. reflections	1879
R_{work} / R_{free}	0.1957 / 0.2187
No. atoms	
Protein	1954
Ligand/ion	12
Water	206
B-factors	
Protein	23.92
Ligand/ion	51.33
Water	34.38
R.m.s. deviations	
Bond lengths (Å)	0.011
Bond angles (°)	1.32

*One crystal was used for the structure. *Values in parentheses are for highest-resolution shell.

Supplementary Table 2 | List of the antibodies used in this study.

Protein	*Species*	*Dilution*	*Cat. No.*
Calnexin	*Rabbit*	*1:4000*	*ab22595 (Abcam)*
ABHD10	*Rabbit*	*1:1000*	*ab214085 (Abcam)*
ABHD10	*Rabbit*	*1:1000*	*HPA036991 (Sigma)*
APT1	*Rabbit*	*1:1000*	*ab91603 (Abcam)*
APT2	*Rabbit*	*1:1000*	*ab151578 (Abcam)*
PRDX5	*Rabbit*	*1:1000*	*17724-1-AP (Proteintech)*
PRDX3	*Rabbit*	*1:1000*	*Ab73349 (Abcam)*
FLAG	*Mouse*	*1:1000*	*MA1-91878 (Invitrogen)*
ALDH6A1	*Mouse*	*1:1000*	*sc-365160 (Santa Cruz Biotechnology)*
Streptavidin-HRP		*1:2000*	*3999S (Cell Signalling Technology)*
Alpha-Tubulin-HRP		*1:2000*	*hrp-66031 (Proteintech)*
Anti Rabbit IgG-HRP	*Goat*	*1:4000*	*7074S (Cell Signalling Technology)*
Anti Mouse IgGk BP-HRP		*1:4000*	*sc-516102 (Santa Cruz Biotechnology)*

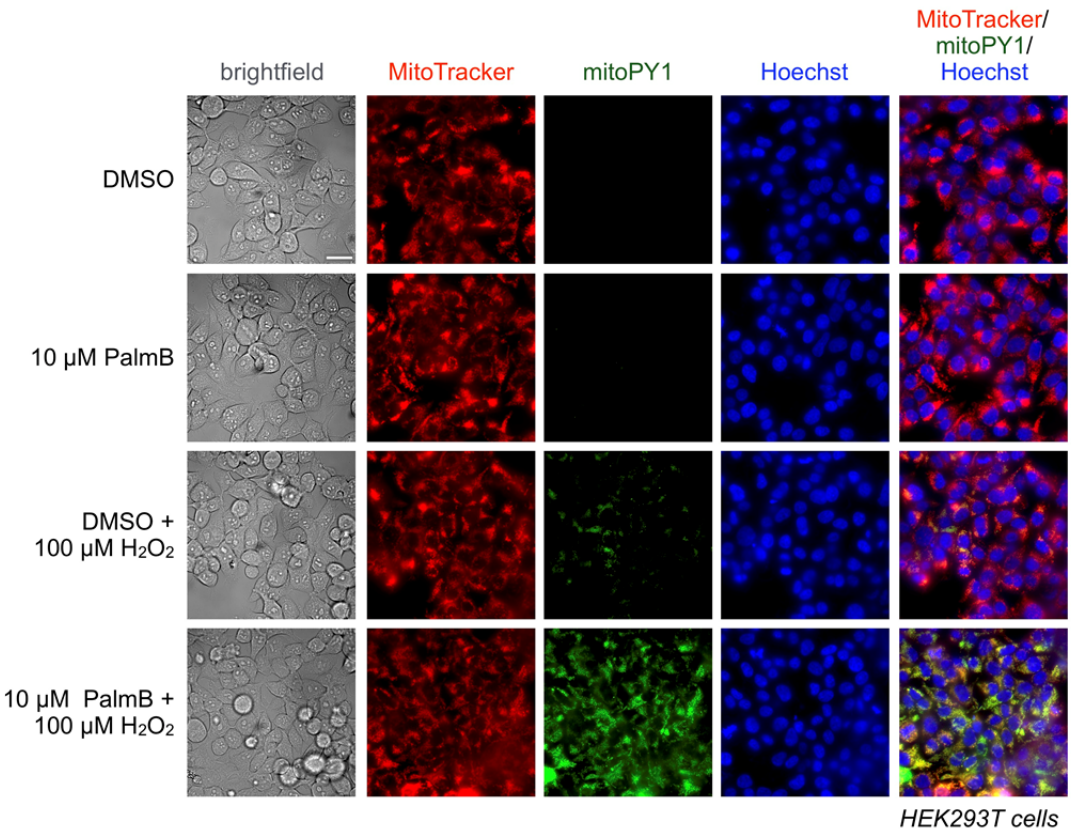

Supplementary Figure 1 | Complete imaging series for Fig 1a. HEK293T cells were treated with 1 μM Hoechst 33342, 100 nM MitoTracker Deep Red, 2 μM mitoPY1 and either DMSO as control or 10 μM PalmB for 30 min. Cells were then washed, loaded with or without 100 μM H_2O_2 for 10 min, and then analyzed by epifluorescence microscopy. Images for brightfield, MitoTracker, mitoPY1, Hoechst 33342 nuclear stain, and an overlay of MitoTracker, mitoPY1, and Hoechst 33342 are shown for each set of conditions. 25 μm scale bar shown. Two biological replicates with similar results were performed.

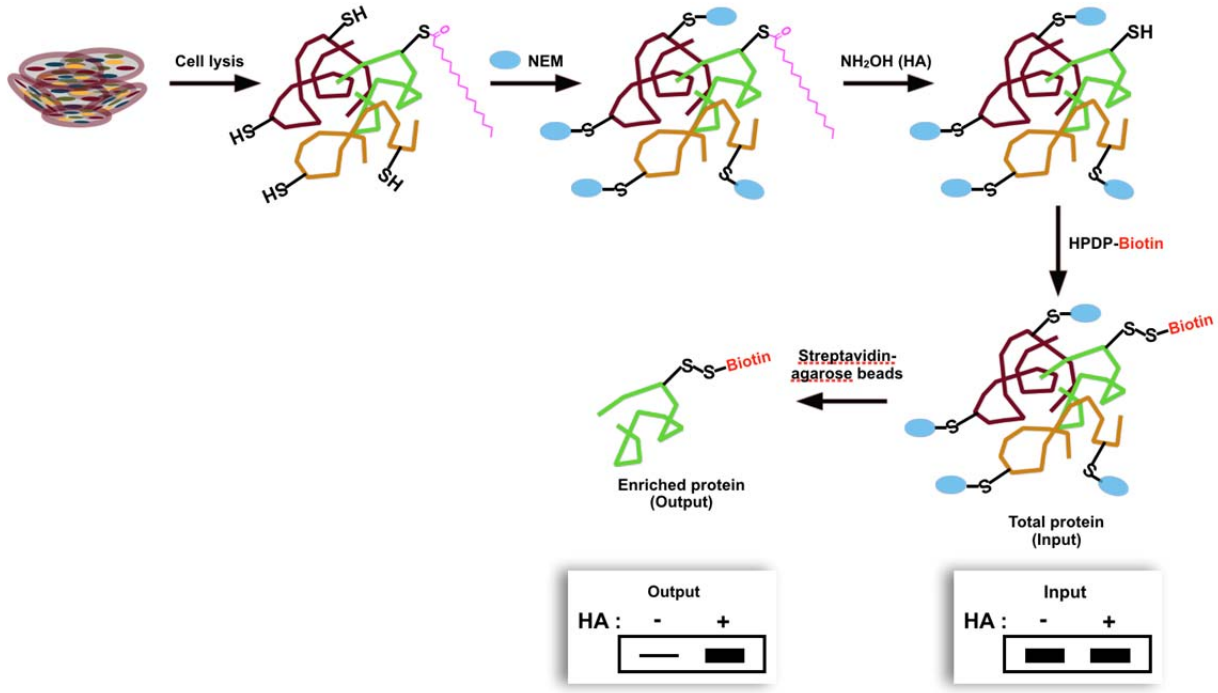

Supplementary Figure 2 | Schematic of ABE assay. Expected pattern of chemiluminiscence signal for input *(right)* and output *(left)* samples are highlighted.

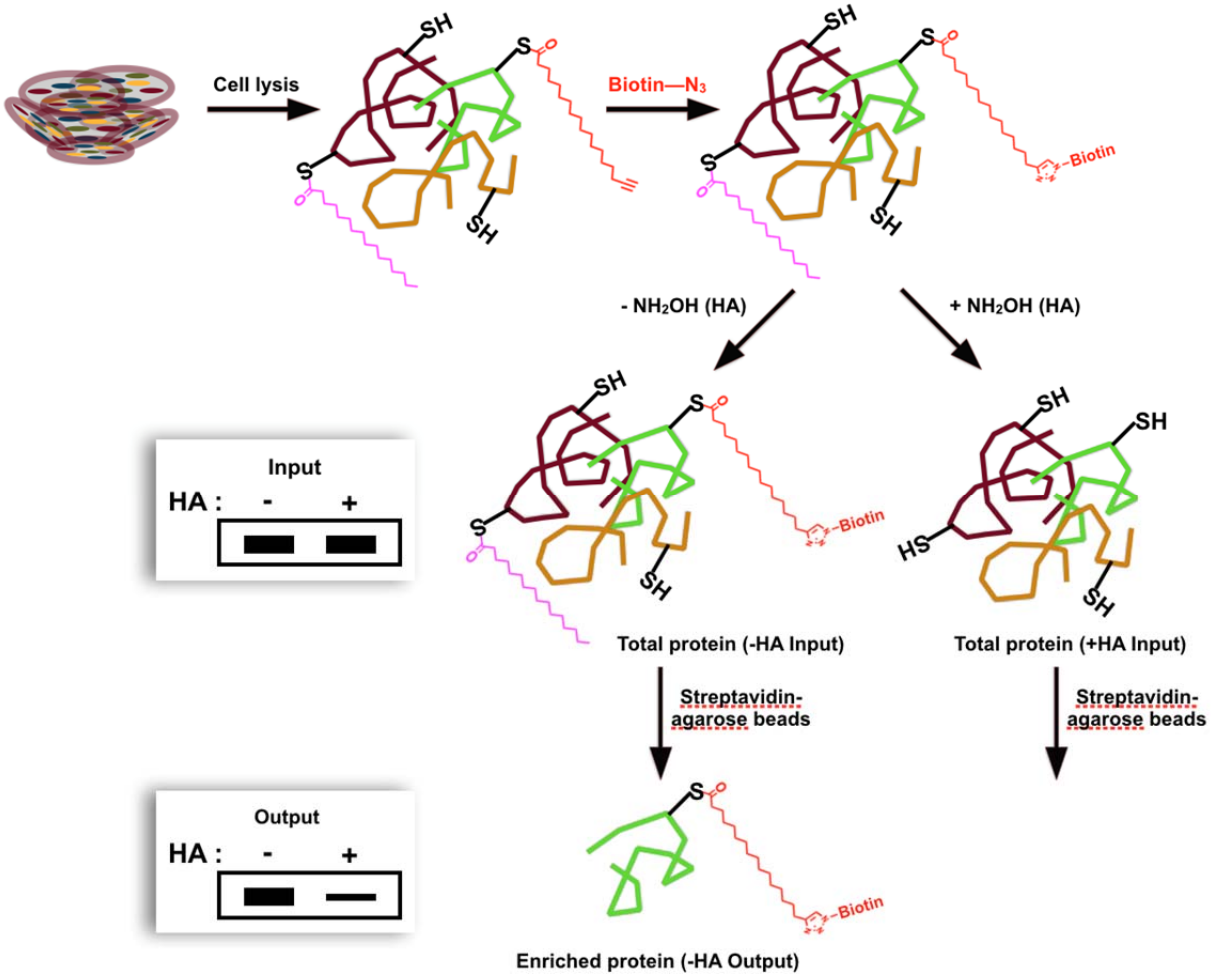

Supplementary Figure 3 | Schematic of metabolic labeling assay. Expected pattern of chemiluminiscence signal for input *(upper)* and output *(bottom)* samples are highlighted.

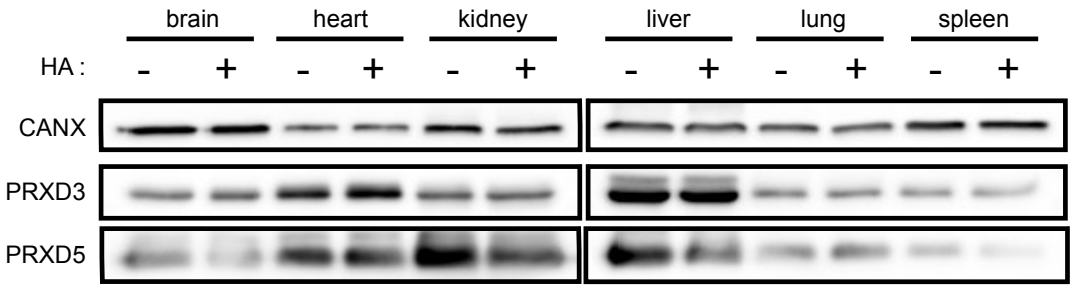

Supplementary Figure 4 | Western blots for input mouse tissue samples before biotinylated-cysteines enrichment for *in vivo* ABE shown in Fig. 1e.

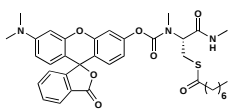

4; DPP-2

- *Structural Feature:*
  Pro-fluorescent probe attached to cysteine analog containing octanoyl thioester
- *Application:*
  Enables live cell imaging of thioesterase activity in the cytosol

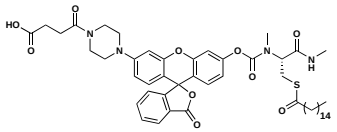

5; DPP-5

- *Structural Feature:*
  Pro-fluorescent probe attached to cysteine analog containing palmitoyl thioester

  Contains anionic functionality which enhances water solubility
- *Application:*
  Enables measuring depalmitoylase activity in vitro and in vivo

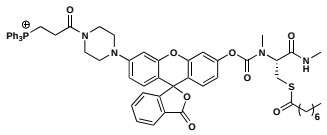

6; MitoDPP-2

- *Structural Feature:*
  Pro-fluorescent probe attached to cysteine analog containing octanoyl thioester

  Contains triphenylphosphonium group which selectively targets probe to mitochondria
- *Application:*
  Enables live cell imaging of thioesterase activity in mitochondria

Supplementary Figure 5 | Compilation of the DPPs (DPP-2[1], DPP-5[2] and mitoDPP-2[3]) used in this study to measure APT activity indicating their key structural features and applications.

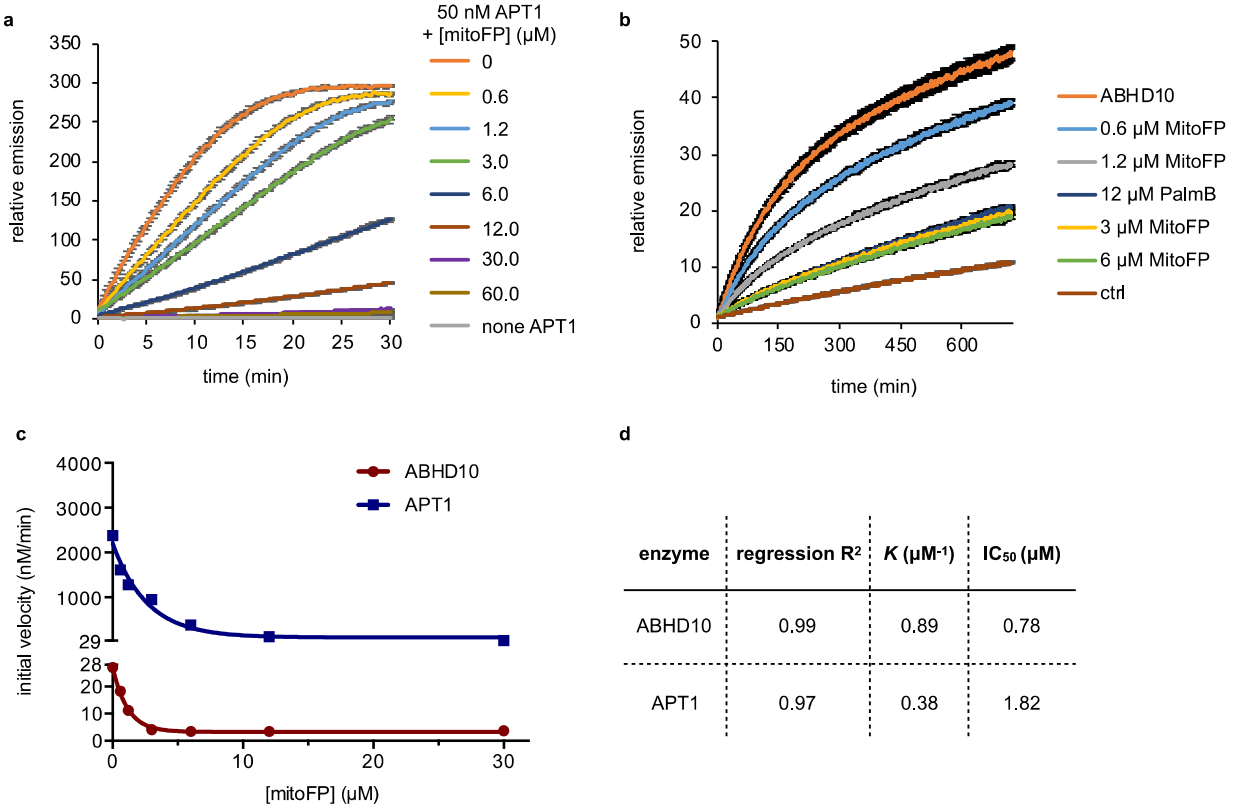

enzyme	regression R^2	K (μM^{-1})	IC_{50} (μM)
ABHD10	0.99	0.89	0.78
APT1	0.97	0.38	1.82

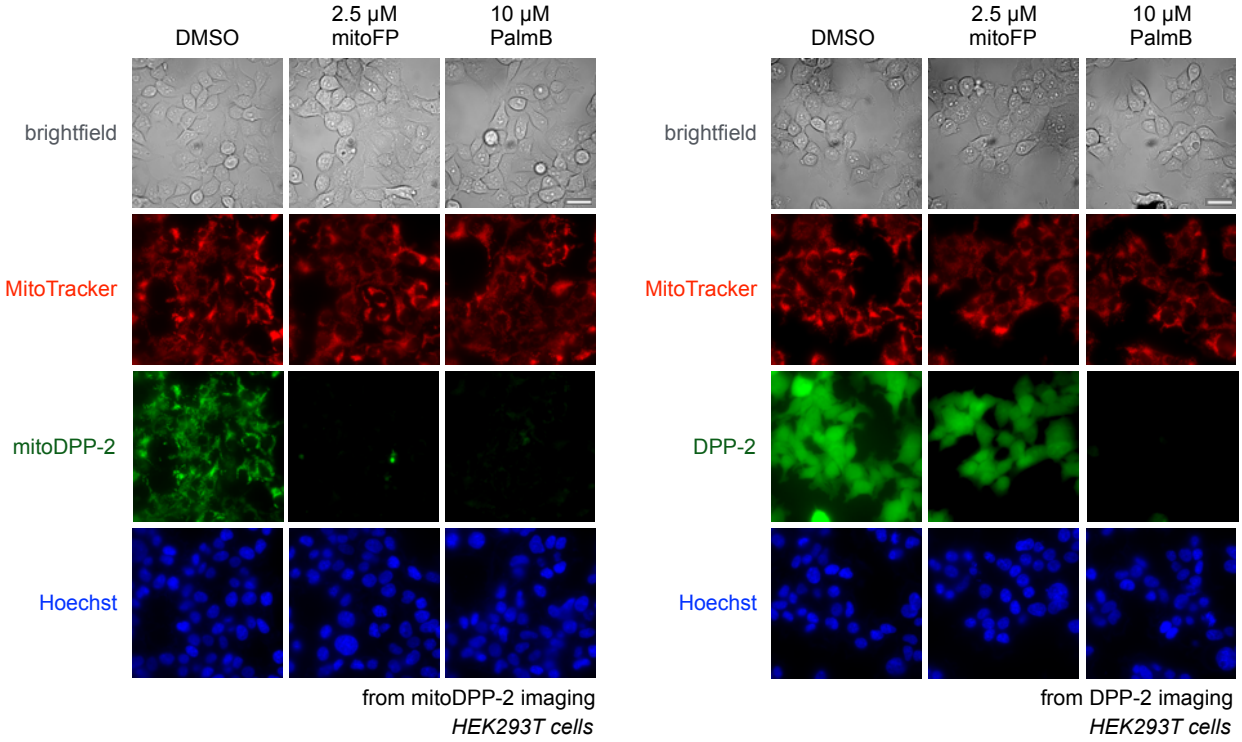

Supplementary Figure 7 | Representative images for comparison of mitoFP potency to deactivate mitochondrial APTs in comarison to PalmB in HEK293T cells shown in figure 2d. HEK293T cells were treated with 1 µM Hoechst 33342, 100 nM MitoTracker Deep Red, and either DMSO as control or 2.5 µM mitoFP or 10 µM PalmB for 30 min. Cells were then washed, loaded with 500 nM mitoDPP-2 (*left*) or 1µM DPP-2 (*right*) for 10 min, and then analyzed by epifluorescence microscopy. Images for brightfield, MitoTracker, mitoDPP-2/DPP-2 and Hoechst 33342 nuclear stain are shown for each set of conditions. 25 µm scale bar shown. Two biological replicates with similar results were performed.

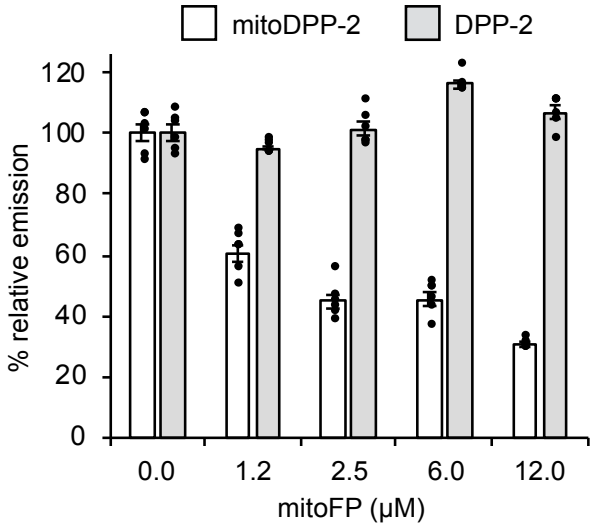

Supplementary Figure 8 | MitoFP-dose-dependent response in HepG2 cells of mitochondrial and cytosolic APTs activity as measured by epifluorescence microscopy using mitoDPP-2 *(black)* and DPP-2 *(grey)*, respectively. Data expressed as mean ± s.e.m. (n = 6 images from two biological replicates), and normalized to control cells treated with DMSO alone.

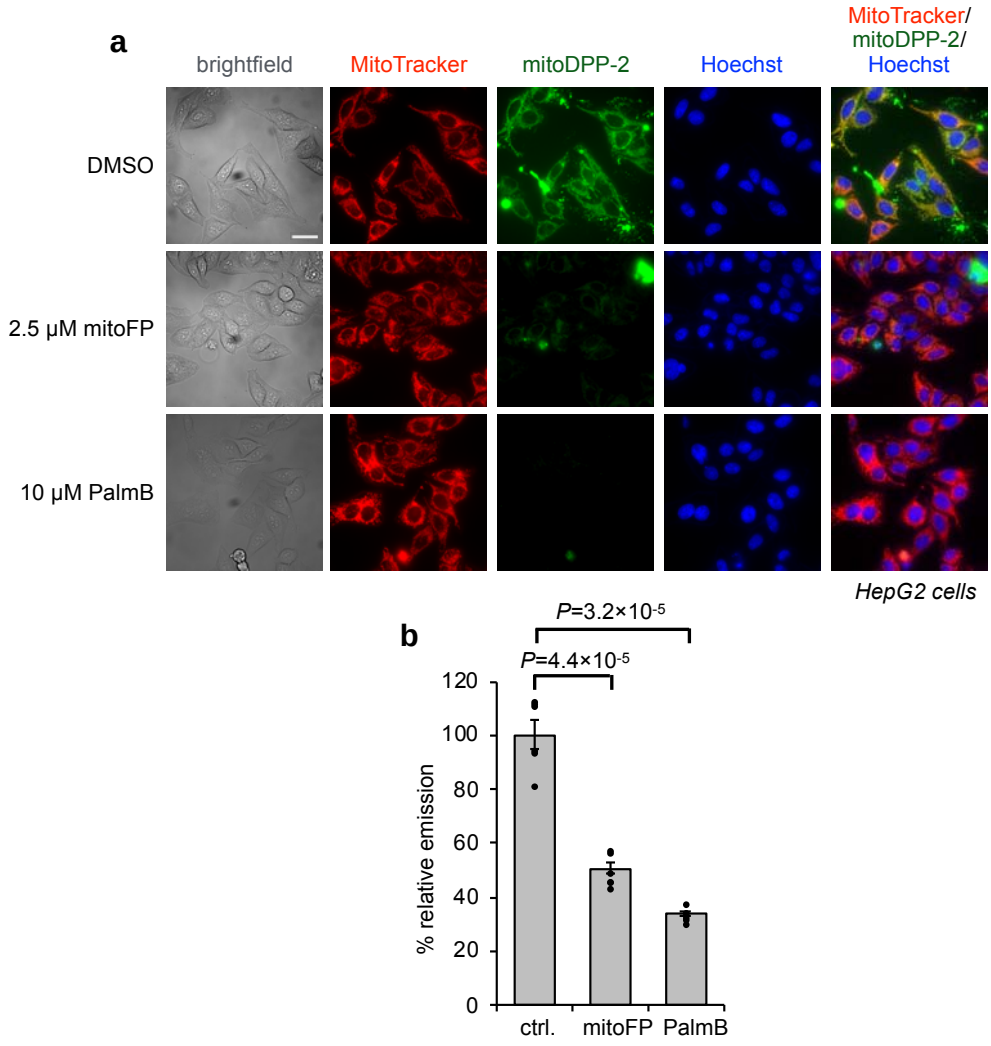

Supplementary Figure 9 | Comparison of mitoFP potency to deactivate mitochondrial APTs in comarison to PalmB in HepG2 cells. (a) HepG2 cells were treated with 1 μM Hoechst 33342, 100 nM MitoTracker Deep Red, and either DMSO as control or 2.5 μM mitoFP or 10 μM PalmB for 30 min. Cells were then washed, loaded with 500 nM mitoDPP-2 for 10 min, and then analyzed by epifluorescence microscopy. Images for brightfield, MitoTracker, mitoDPP-2, Hoechst 33342 nuclear stain, and an overlay of MitoTracker, mitoDPP-2, and Hoechst 33342 are shown for each set of conditions. 25 μm scale bar shown. **(b)** Quantification of the relative fluorescence intensity from mitoDPP-2 in set of conditions shown in **a**. Statistical analyses performed with a two-tailed Student's *t*-test with unequal variance (n = 6 images from two biological replicates). Data expressed as mean ± s.e.m. and normalized to control cells treated with DMSO alone.

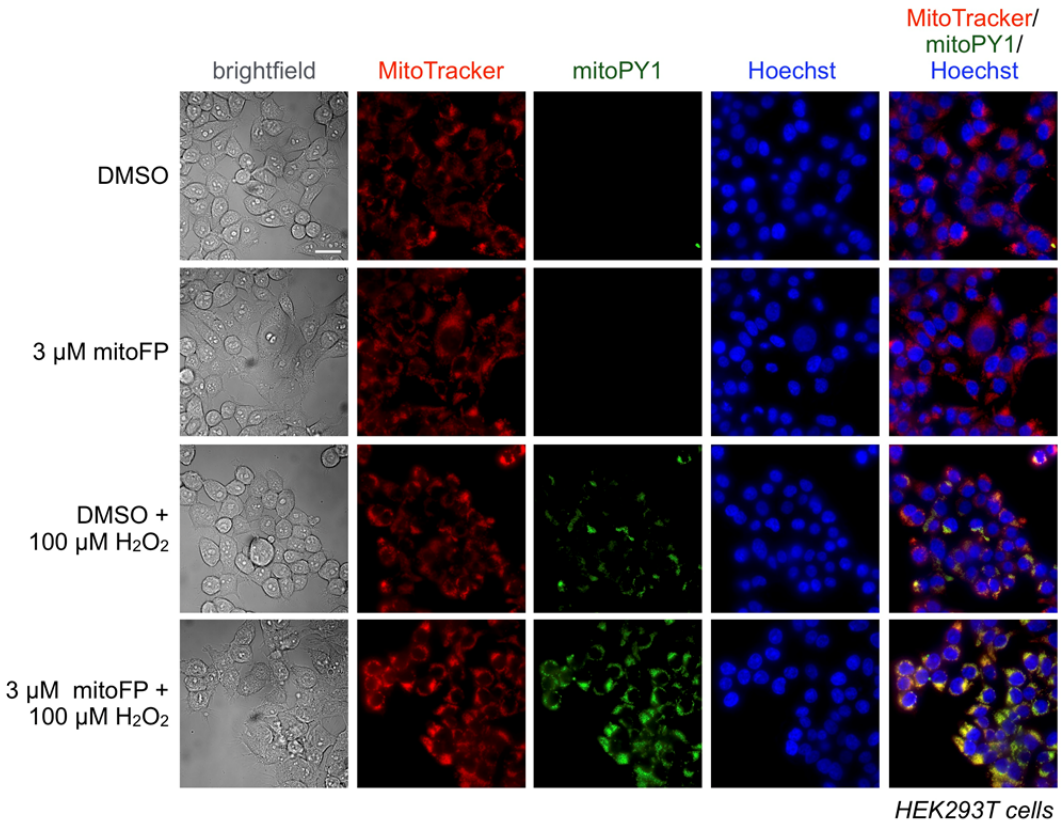

Supplementary Figure 10 | Representative images for Fig 2e. HEK293T cells were treated with 1 μM Hoechst 33342, 100 nM MitoTracker Deep Red, 2 μM mitoPY1 and either DMSO as control or 3 μM mitoFP for 30 min. Cells were then washed, loaded with or without 100 μM H_2O_2 for 10 min, and then analyzed by epifluorescence microscopy. Images for brightfield, MitoTracker, mitoPY1, Hoechst 33342 nuclear stain, and an overlay of MitoTracker, mitoPY1, and Hoechst 33342 are shown for each set of conditions. 25 μm scale bar shown. Two biological replicates with similar results were performed.

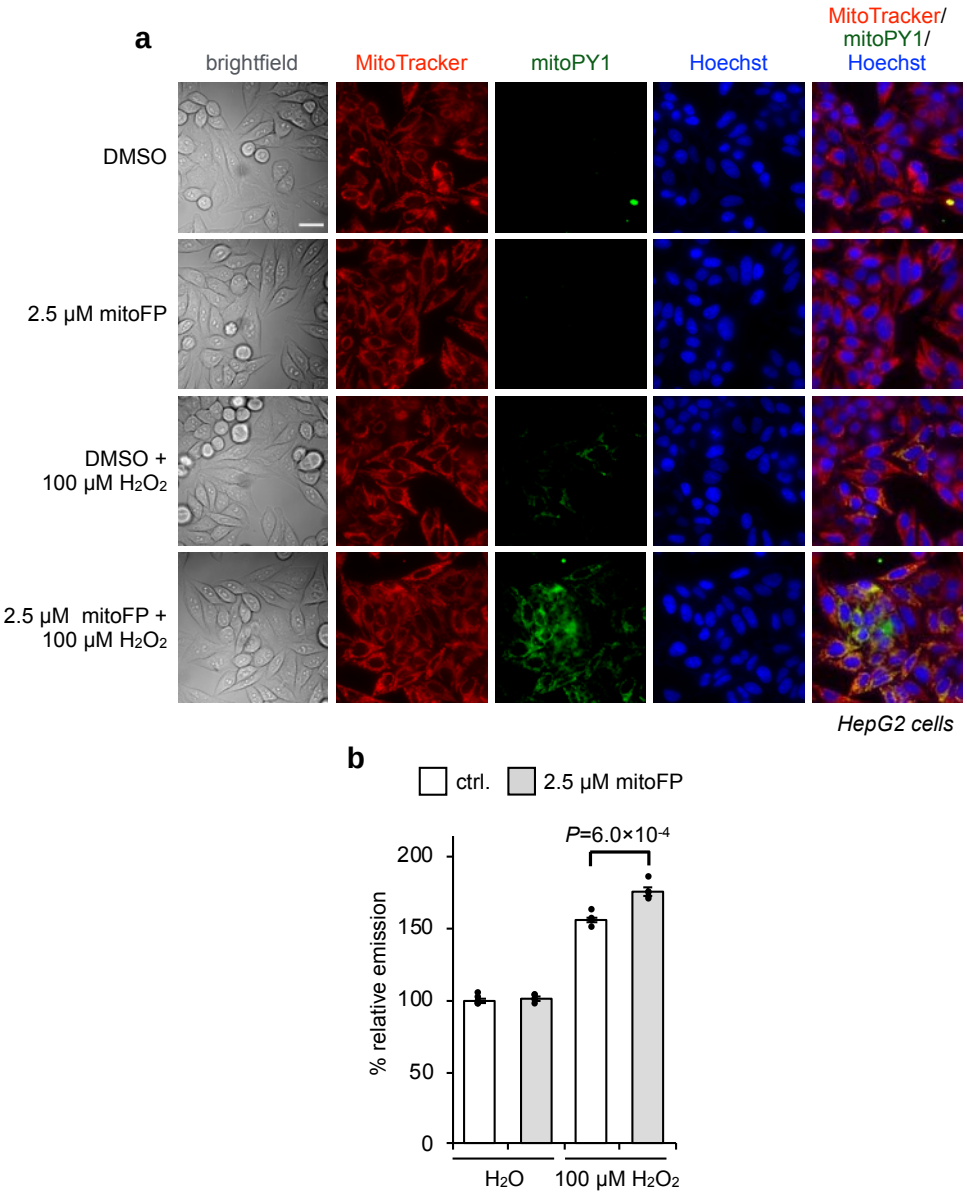

Supplementary Figure 11 | MitoFP diminishes mitochondrial redox buffering capacity in HepG2 cells. (**a**) HepG2 cells were treated with 1 μM Hoechst 33342, 100 nM MitoTracker Deep Red, 2 μM mitoPY1 and either DMSO as control or 2.5 μM mitoFP for 30 min. Cells were then washed, loaded with or without 100 μM H_2O_2 for 10 min, and then analyzed by epifluorescence microscopy. Images for brightfield, MitoTracker, mitoPY1, Hoechst 33342 nuclear stain, and an overlay of MitoTracker, mitoPY1, and Hoechst 33342 are shown for each set of conditions. 25 μm scale bar**.** (**b**) Quantification of the relative fluorescence intensity from mitoPY1 in each set of conditions shown in **a**. Statistical analyses performed with a two-tailed Student's *t*-test with unequal variance (n = 5 images). Data expressed as mean ± s.e.m. and

normalized to control cells treated with DMSO alone. Two biological replicates with similar results were performed.

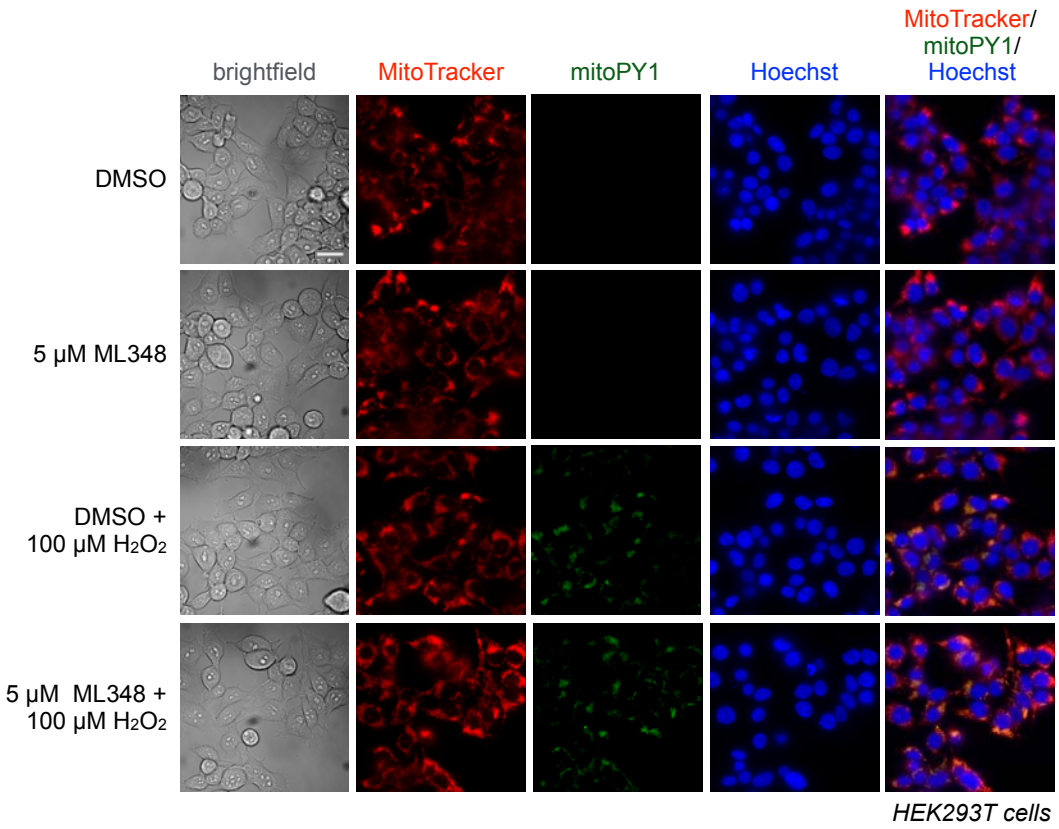

Supplementary Figure 12 | Representative images for Fig 2f. HEK293T cells were treated with 1 μM Hoechst 33342, 100 nM MitoTracker Deep Red, 2 μM mitoPY1 and either DMSO as control or 5 μM ML348 for 30 min. Cells were then washed, loaded with or without 100 μM H_2O_2 for 10 min, and then analyzed by epifluorescence microscopy. Images for brightfield, MitoTracker, mitoPY1, Hoechst 33342 nuclear stain, and an overlay of MitoTracker, mitoPY1, and Hoechst 33342 are shown for each set of conditions. 25 μm scale bar shown. Two biological replicates with similar results were performed.

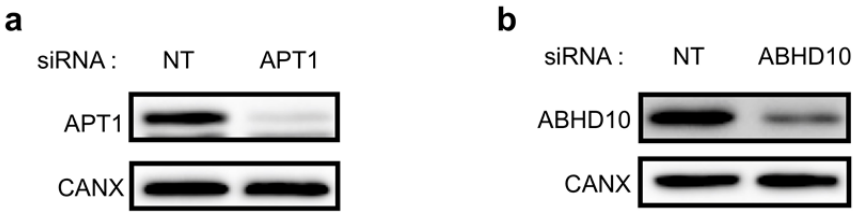

Supplementary Figure 13 | Knockdown efficiency of APT1 (a) **and ABHD10** (b) **analyzed by western blots**. Calnexin *(CANX)* used as loading control. *NT:* Non-targeting siRNA. N ≥ 3 biological replicates were performed.

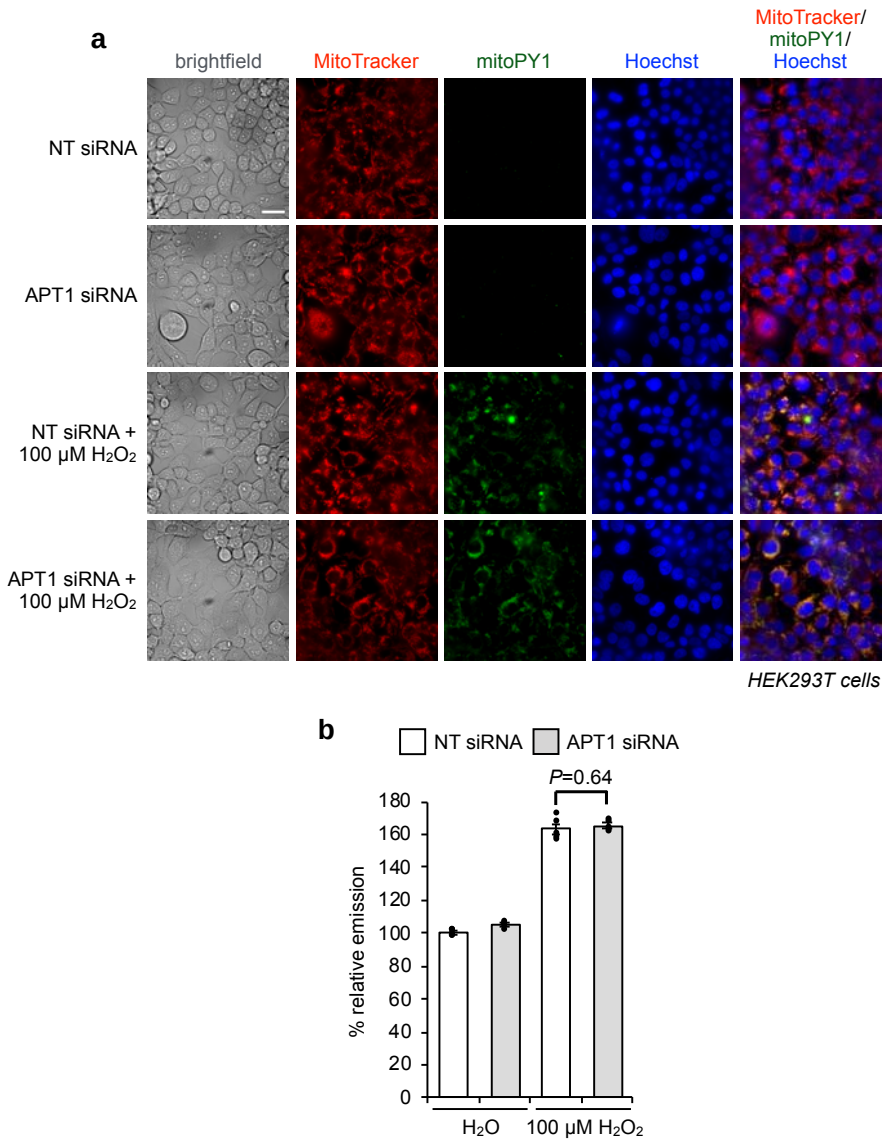

Supplementary Figure 14 | APT1 knockdown does not alter mitochondrial redox buffering capacity in HEK293T cells. (**a**) HEK293T cells transfected with NT siRNA or APT1 siRNA were treated with 1 μM Hoechst 33342, 100 nM MitoTracker Deep Red, and 2 μM mitoPY1 for 30 min. Cells were then washed, loaded with or without 100 μM H_2O_2 for 10 min, and then analyzed by epifluorescence microscopy. Images for brightfield, MitoTracker, mitoPY1, Hoechst 33342 nuclear stain, and an overlay of MitoTracker, mitoPY1, and Hoechst 33342 are shown for each set of conditions. 25 μm scale bar**.** (**b**) Quantification of the relative fluorescence intensity from mitoPY1 in each set of conditions shown in **a**. Statistical analyses performed with a two-tailed Student's *t*-test with unequal variance (n = 5 images). Data expressed as mean ± s.e.m. and normalized to unstimulated control cells treated with NT siRNA. Two biological replicates with similar results were performed.

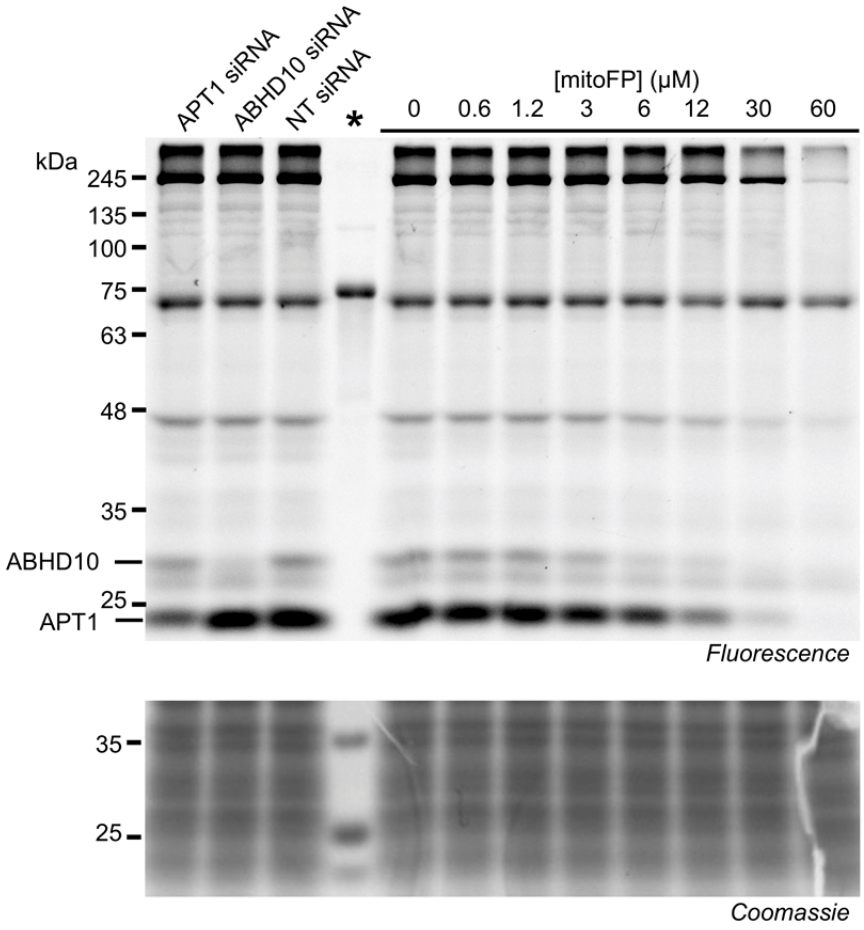

Supplementary Figure 15 | Full gels of Fig. 3c. Competitive ABPP (*upper panel*) in siRNA treated HEK293T cells (1-3 lanes from left) confirms the bands representing APT1 and ABHD10. Lanes 5-12 (from left) are shown in Fig. 3c. Coomassie staining *(lower panel)* is used to assess protein amount loaded. The asterisk shows the marker lane. Two biological replicates with similar results were performed.

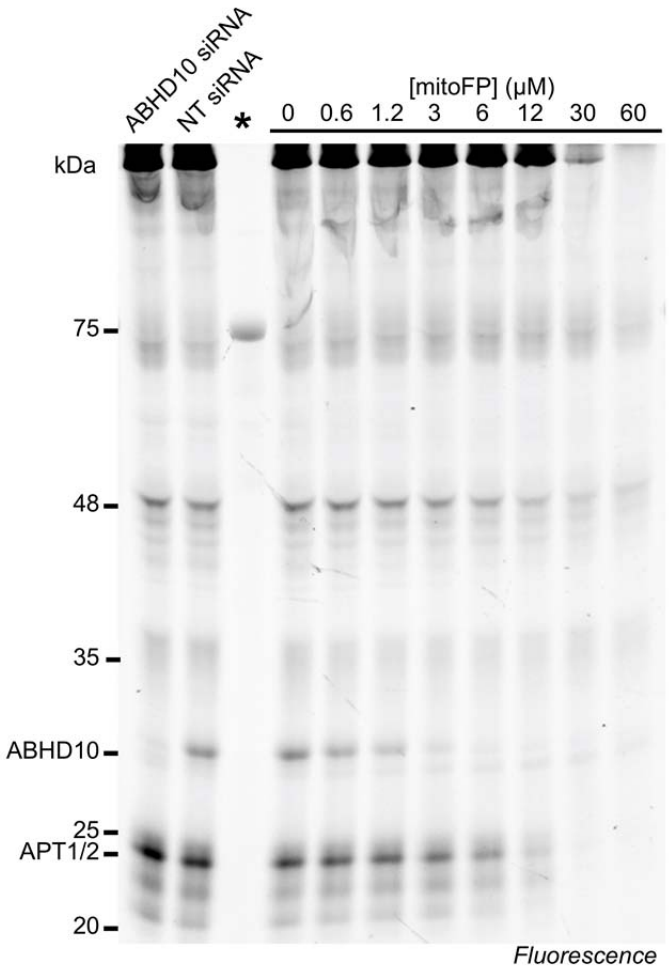

Supplementary Figure 16 | Competitive ABPP in siRNA treated HepG2 cells (first two lanes from left) confirms the bands representing ABHD10. Lanes 4-11 (from left) show that mitoFP inhibits ABHD10 in a dose-dependent manner. The asterisk shows the marker lane. Two biological replicates with similar results were performed.

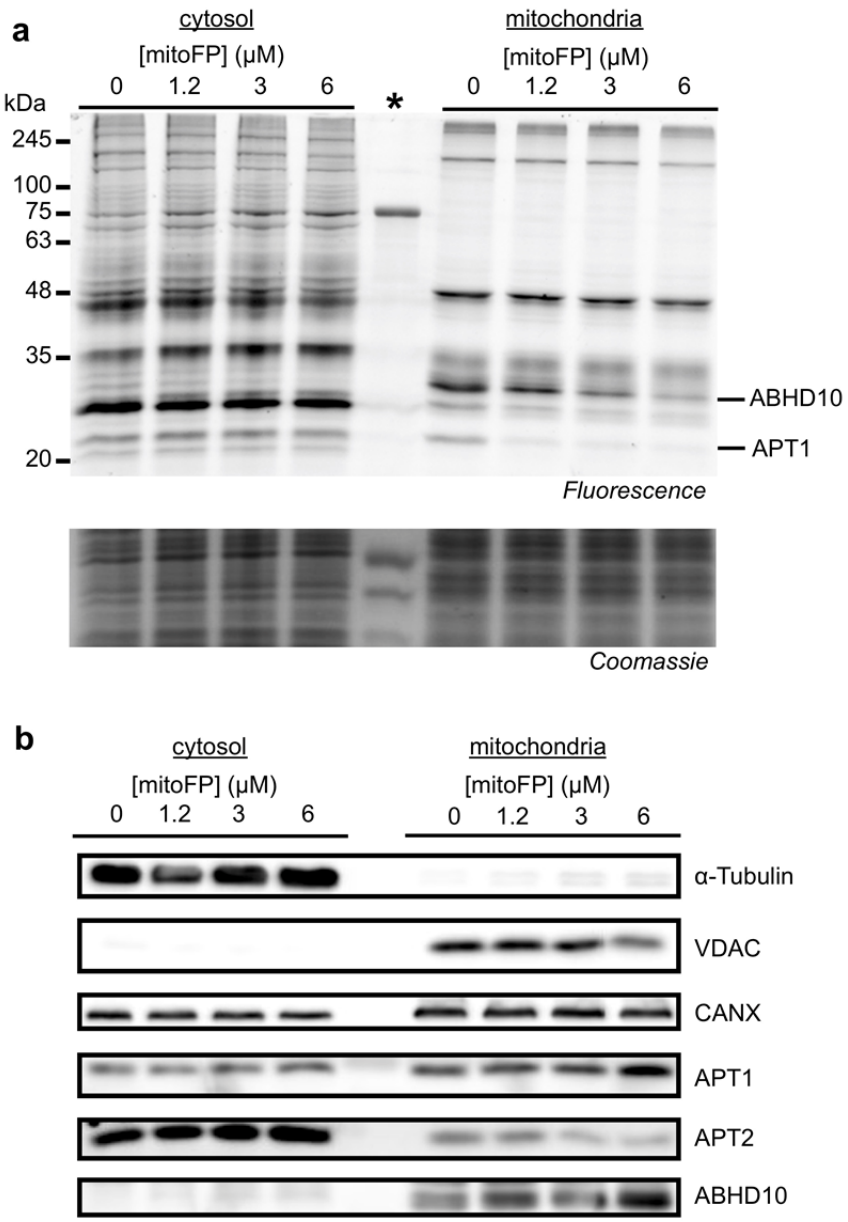

Supplementary Figure 17 | (**a**) Competitive ABPP (*upper panel*) to examine *cytosolic* and *mitochondrial* serine hydrolase targets of mitoFP in HepG2 cells. Coomassie staining *(lower panel)* is used as loading control. Asterisk indicates the marker lane. (**b**) Western blot analysis to examine purity of *cytosolic* and *mitochondrial* fractions from **a**. High VDAC indicates that fractions are highly enriched for mitochondria. Two biological replicates with similar results were performed.

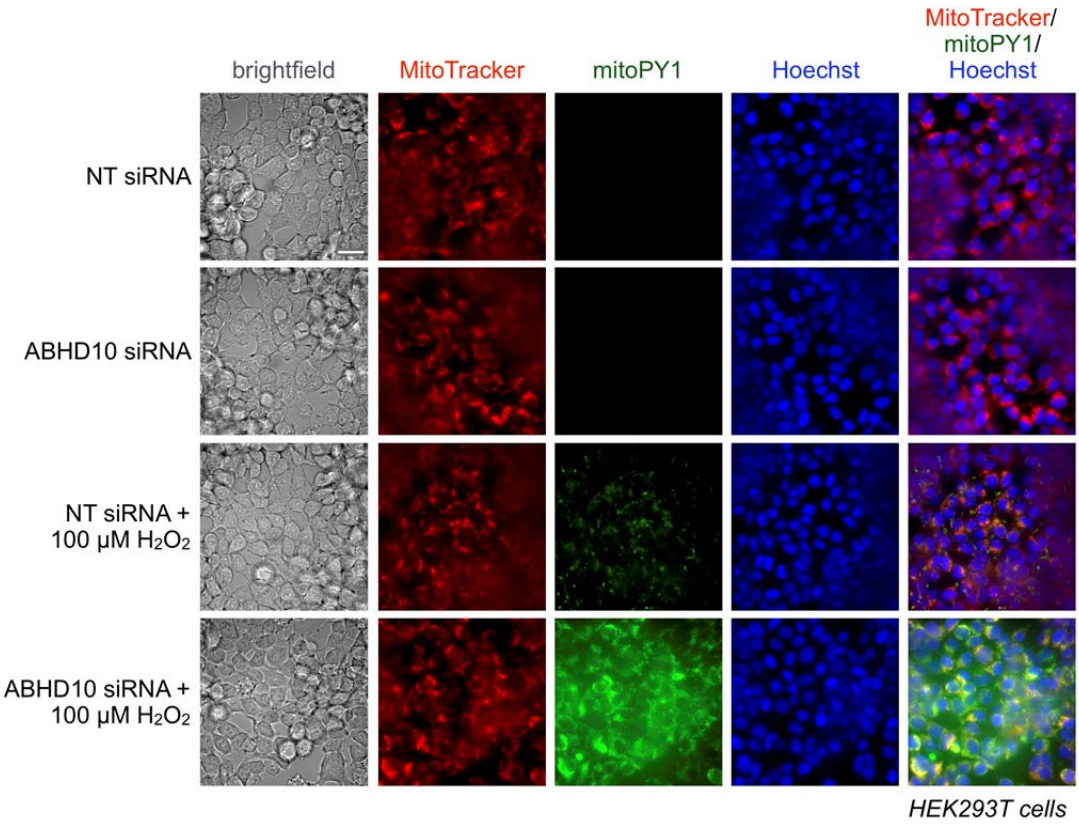

Supplementary Figure 18 | Complete imaging series for Fig 3d. HEK293T cells transfected with control or ABHD10 siRNA were treated with 1 μM Hoechst 33342, 100 nM MitoTracker Deep Red, and 2 μM mitoPY1 for 30 min. Cells were then washed, loaded with or without 100 μM H_2O_2 for 10 min, and then analyzed by epifluorescence microscopy. Images for brightfield, MitoTracker, mitoPY1, Hoechst 33342 nuclear stain, and an overlay of MitoTracker, mitoPY1, and Hoechst 33342 are shown for each set of conditions. 25 μm scale bar shown. Three biological replicates with similar results were performed.

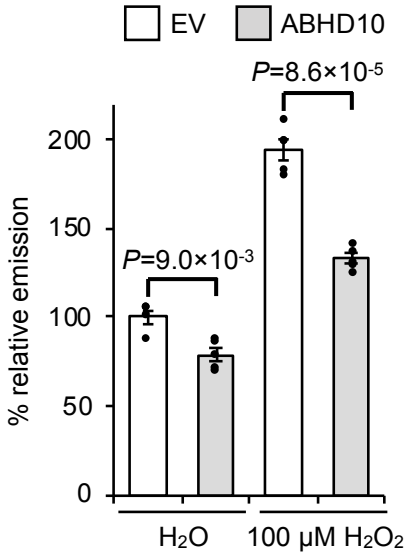

Supplementary Figure 19 | ABHD10 overexpression increases mitochondrial redox buffering capacity in HEK293T cells. HEK293T cells trasfected with empty vector *(vector)* control or ABHD10 were treated with 1 μM Hoechst 33342, 100 nM MitoTracker Deep Red, and 2 μM mitoPY1 for 30 min. Cells were then washed, loaded with or without 100 μM H_2O_2 for 10 min, and then analyzed by epifluorescence microscopy**.** Quantification of the relative fluorescence intensity from mitoPY1 in each set of conditions. Statistical analyses performed with a two-tailed Student's *t*-test with unequal variance (n = 5 images except 4 images for unstimulated control). Data expressed as mean ± s.e.m. and normalized to unstimulated control cells treated with empty vector.

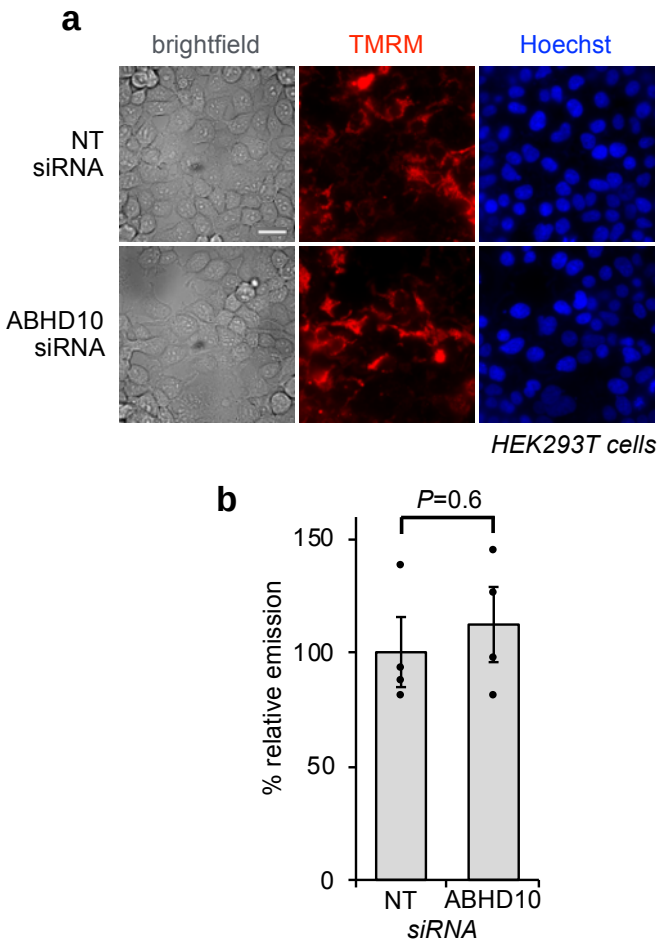

Supplementary Figure 20 | ABHD10 knockdown does not alter mitochondrial membrane potential. (**a**) HEK293T cells transfected with control or ABHD10 siRNA were treated with 1 μM Hoechst 33342, and 100 nM TMRM for 30 min. Cells were then washed, and then analyzed by epifluorescence microscopy. Images for brightfield, Hoechst 33342 nuclear stain, and TMRM are shown for each set of conditions. 25 μm scale bar shown. (**b**) Quantification of the relative fluorescence intensity from TMRM in each set of conditions shown in **a**. Data expressed as mean ± s.e.m. (n = 4 images), and normalized to control cells treated with NT siRNA.

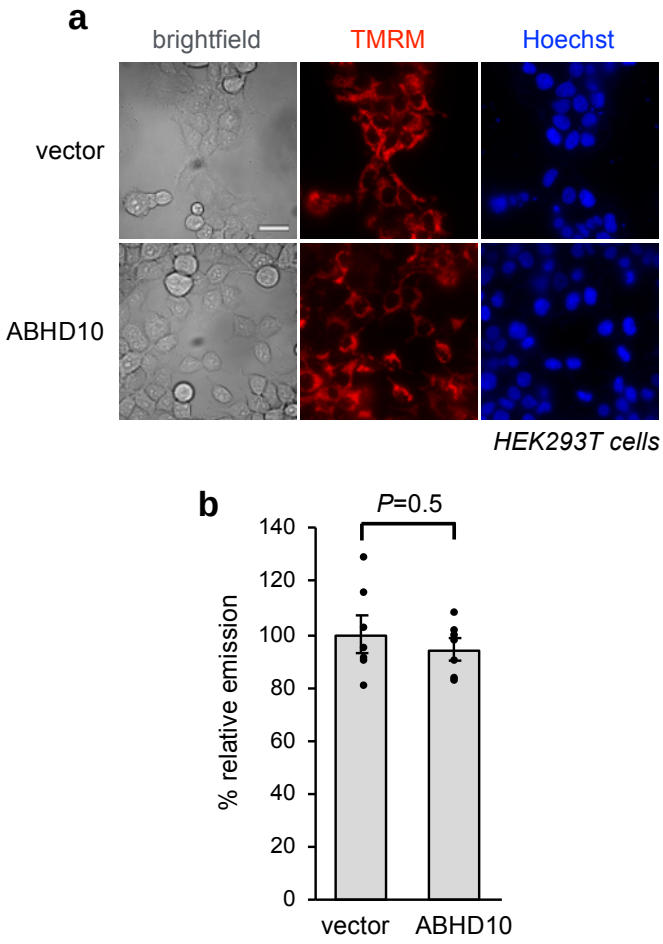

Supplementary Figure 21 | ABHD10 overexpression does not alter mitochondrial membrane potential. (**a**) HEK293T cells transfected with empty vector *(vector)* or ABHD10 expression plasmids were treated with 1 μM Hoechst 33342, and 100 nM TMRM for 30 min. Cells were then washed, and then analyzed by epifluorescence microscopy. Images for brightfield, Hoechst 33342 nuclear stain, and TMRM are shown for each set of conditions. 25 μm scale bar shown. (**b**) Quantification of the relative fluorescence intensity from TMRM in each set of conditions shown in **a**. Data expressed as mean ± s.e.m. (n = 7 images), and normalized to control cells transfected with empty vector.

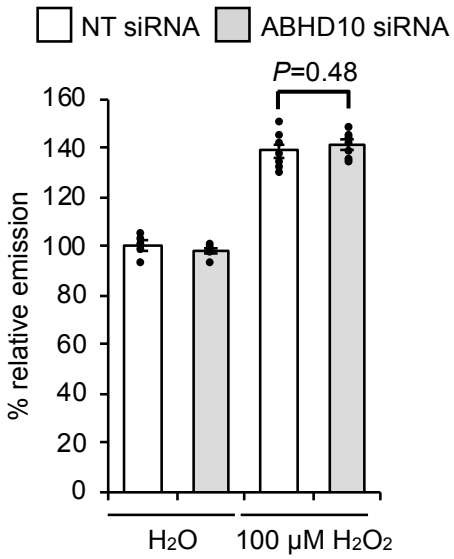

Supplementary Figure 22 | ABHD10 knockdown does not alter cytoplasmic redox buffering capacity in HEK293T cells. HEK293T cells trasfected with contol or ABHD10 siRNA were treated with 1 μM Hoechst 33342, 100 nM MitoTracker Deep Red, and 5 μM PY1 for 30 min. Cells were then washed, loaded with or without 100 μM H_2O_2 for 13 min, and then analyzed by epifluorescence microscopy. Quantification of the relative fluorescence intensity from PY1 in each set of conditions shown. Statistical analyses performed with a two-tailed Student's *t*-test with unequal variance (n = 5 and 7 images for unstimulated and stimulated cells, respectively). Data expressed as mean ± s.e.m. and normalized to unstimulated control cells treated with NT siRNA.

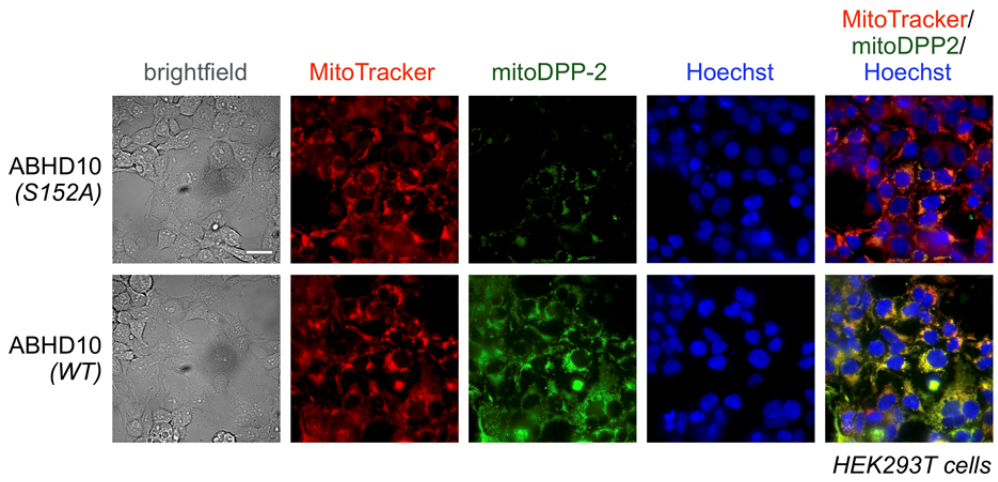

Supplementary Figure 23 | Complete imaging series for Fig 4a. HEK293T cells transfected with ABHD10 *(WT)* and ABHD10 *(S152A)* plasmids were treated with 1 μM Hoechst 33342 and 100 nM MitoTracker Deep Red for 30 min. Cells were then washed, loaded with 500 nM mitoDPP-2 for 10 min, and then analyzed by epifluorescence microscopy. Images for brightfield, MitoTracker, mitoDPP-2, Hoechst 33342 nuclear stain, and an overlay of MitoTracker, mitoDPP-2, and Hoechst 33342 are shown for each set of conditions. 25 μm scale bar shown. Two biological replicates with similar results were performed.

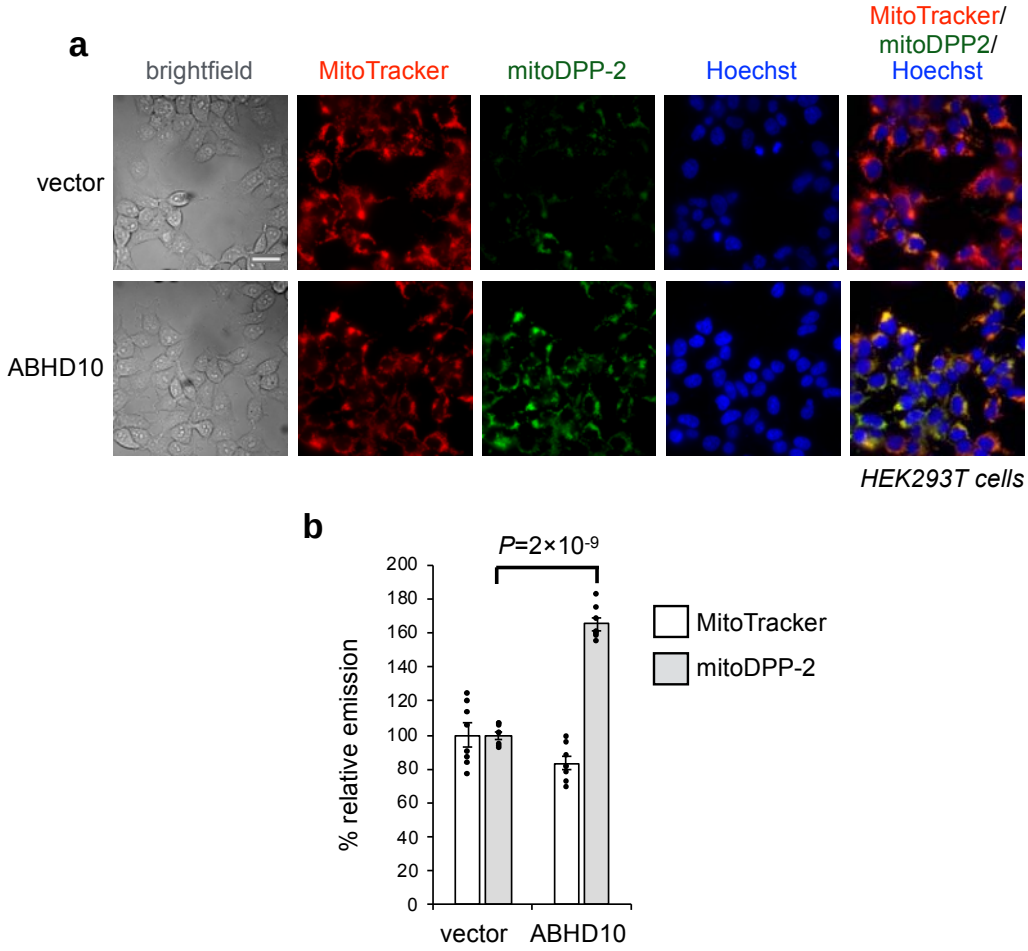

Supplementary Figure 24 | (**a**) HEK293T cells transfected with ABHD10 *(WT)* and empty vector *(vector)* plasmids were treated with 1 μM Hoechst 33342 and 100 nM MitoTracker Deep Red for 30 min. Cells were then washed, loaded with 500 nM mitoDPP-2 for 10 min, and then analyzed by epifluorescence microscopy. Images for brightfield, MitoTracker, mitoDPP-2, Hoechst 33342 nuclear stain, and an overlay of MitoTracker, mitoDPP-2, and Hoechst 33342 are shown for each set of conditions. 25 μm scale bar shown. (**b**) Quantification of relative fluorescence intensities in from MitoTracker *(black)* and mitoDPP-2 *(grey)* in each set of conditions. Statistical analyses performed with a two-tailed Student's *t*-test with unequal variance (n = 8 images from two biological replicates). Data expressed as mean ± s.e.m. and normalized to control cells transfected with empty vector.

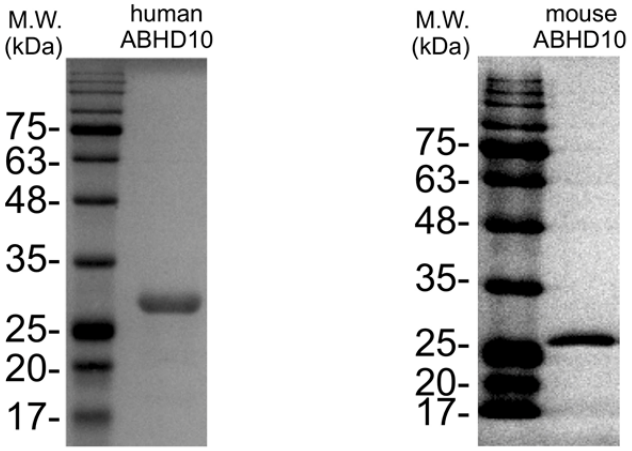

Supplementary Figure 25 | SDS-PAGE analysis of purified mature human and mouse ABHD10. 3 independent tests with similar results were done.

a

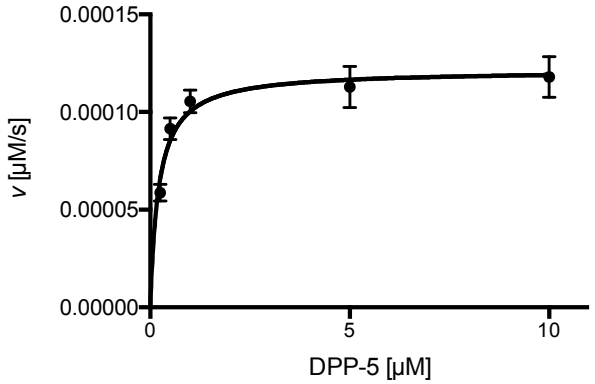

b

enzyme	K_M (µM)	k_{cat} (s^{-1})	k_{cat}/K_M (M^{-1} s^{-1})
APT1	1.6	0.044	2.8×10^4
APT2	2.1	0.066	3.1×10^4
ABHD10	0.21	0.00024	1.1×10^3

Supplementary Figure 26 | (**a**) Michaelis-Menten kinetics regression of ABHD10 (500 nM) enzymatic kinetics at 37 ˚C with DPP-5 as its substrate. Data expressed as mean ± s.e.m. (n = 4)**.** (**b**) Kinetic parameters comparison of APT1, APT2,[2] and ABHD10 at 37 ˚C with substrate DPP-5.

a

```
Human ABHD10| TSLSFLNRPDLPNLAYKKLKGKSPGIIFIPGYLSYMNGTKALAIEEFCKSLGHACIRFDY
Mouse ABHD10| ASLSFLNRSELPNLAYKRLKGKTPGIIFIPGYLSNMNGIKAVAVEEFCKSLGHAFIRFDY

Human ABHD10| SGVGSSDGNSEESTLGKWRKDVLSIIDDLADGPQILVGSSLGGWLMLHAAIARPEKVVAL
Mouse ABHD10| SGIGSSDGNLAECTVGKWRKDVLSILDDVAEGPQILVGSSLGGWLMLHAAIARPEKVIAL

Human ABHD10| IGVATAADTLVTKFNQLPVELKKEVEMKGVWSMPSKYSEEGVYNVQYSFIKEAEHHCLLH
Mouse ABHD10| IGIATAADGLVTQYHALPVETQKEIEMKGEWTLPSRYNKEGYFRIPYSFIKEAEHHCLLH

Human ABHD10| SPIPVNCPIRLLHGMKDDIVPWHTSMQVADRVLSTDVDVILRKHSDHRMREKADIQLLVY
Mouse ABHD10| SPIPVTCPVRLLHGMKDEIVPWQRSLQVADRIVSPDVDVILRKQGDHRMKEKADIHLLIC

Human ABHD10| TIDDLIDKLSTIVN
Mouse ABHD10| TIDDLIDKLS----
```

b

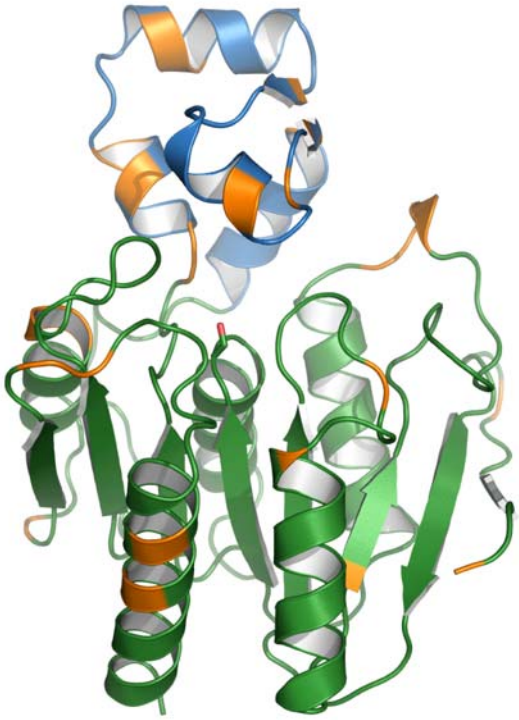

Supplementary Figure 27 (**a**) Sequence alignment between mitochondrial-transit-peptide-cleaved mouse and human ABHD10. The black bold amino acid positions are different between mouse and human, while the gray bold positions are different but similar. The blue rectangle circles the “cap” domain sequences. (**b**) Structural view for the positions of different residues (orange), the blue incidates the “cap” domain.

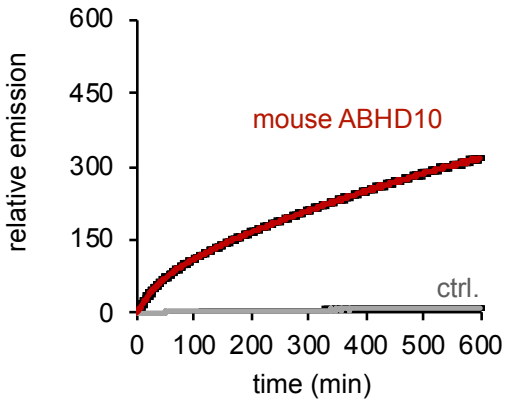

Supplementary Figure 28 | *In vitro* kinetic assay showing *S*-depalmitoylation activity of mature mouse ABHD10 (500 nM, *red*) compared to control without added enzyme *(grey)* as measured using DPP-5 (5 μM). Data expressed as mean ± s.e.m (n=4) and normalized to relative emission of control at *t = 0.*

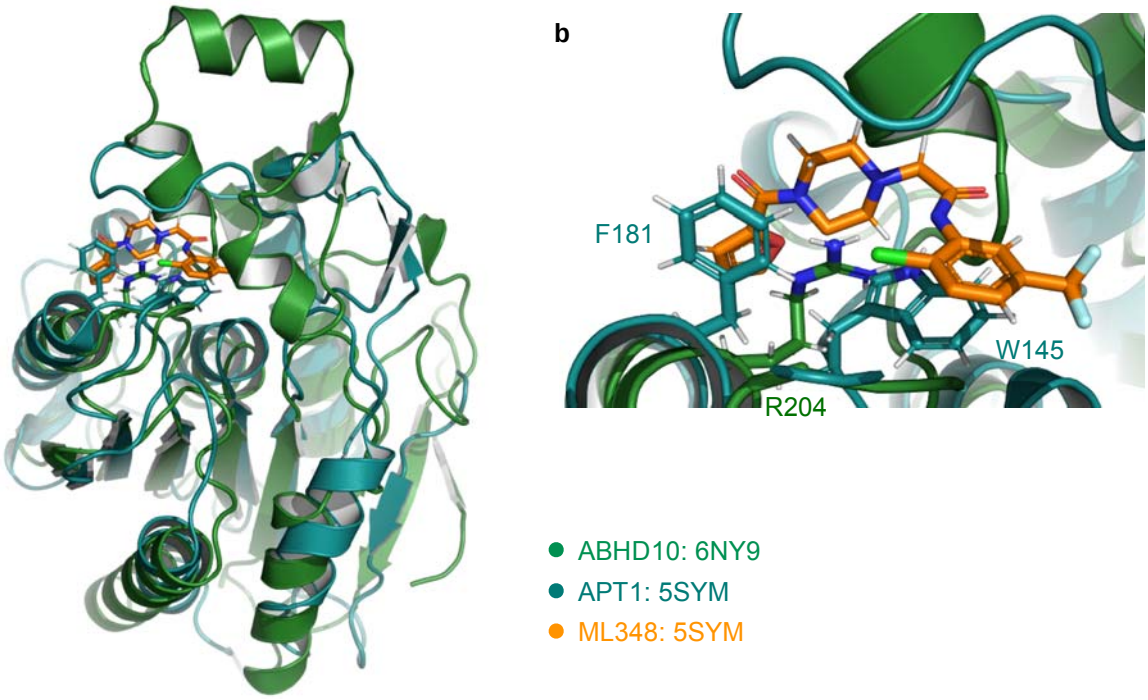

Supplementary Figure 29 | (a) Structure alignment between mouse ABHD10 (*green*, PDB: 6NY9) and inhibitor-bound APT1 (*teal*, PDB: 5SYM). **(b)** Zoomed-in view of the pocket in **a** where ML348 (*orange*) binds. In APT1, the residues F181 and W145 offer *π-π* stacking interaction with ML348, which is lacking in ABHD10 and replaced by R204. This could possibly explain the ML348 selection of APT1 over ABHD10.

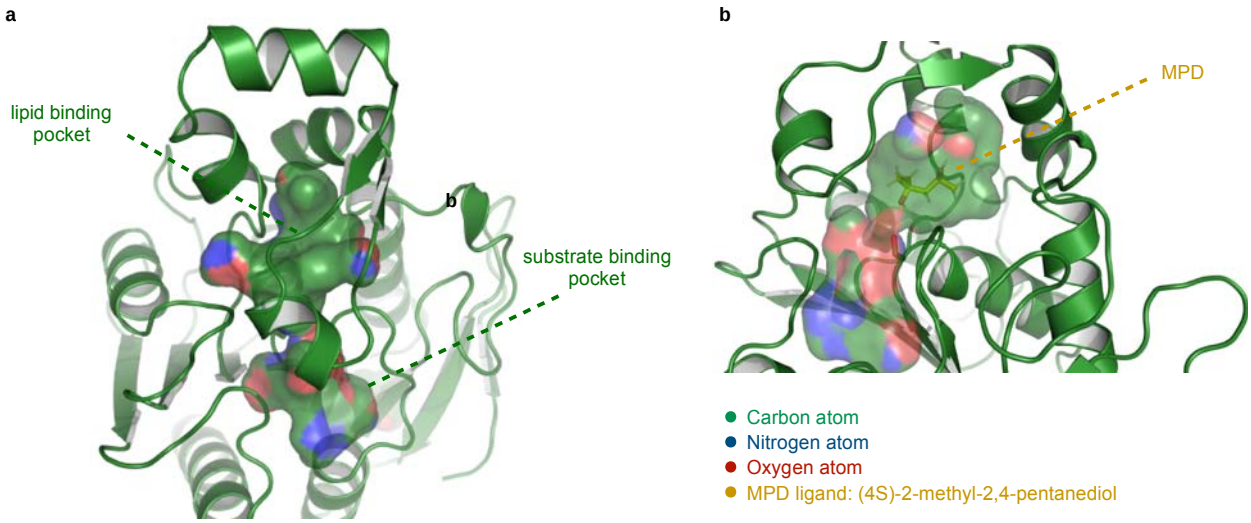

Supplementary Figure 30 | (a) Binding pockets of mouse ABHD10, shown with green as carbon atoms, blue as nitrogen atoms and red as oxygen atoms. The putative lipid binding pocket has more surrounding hydrophobic residues than the putative substrate binding pocket. **(b)** Zoomed-in view showing the bound MPD ligand *(yellow)* in putative lipid binding pocket from the crystallization liquor.

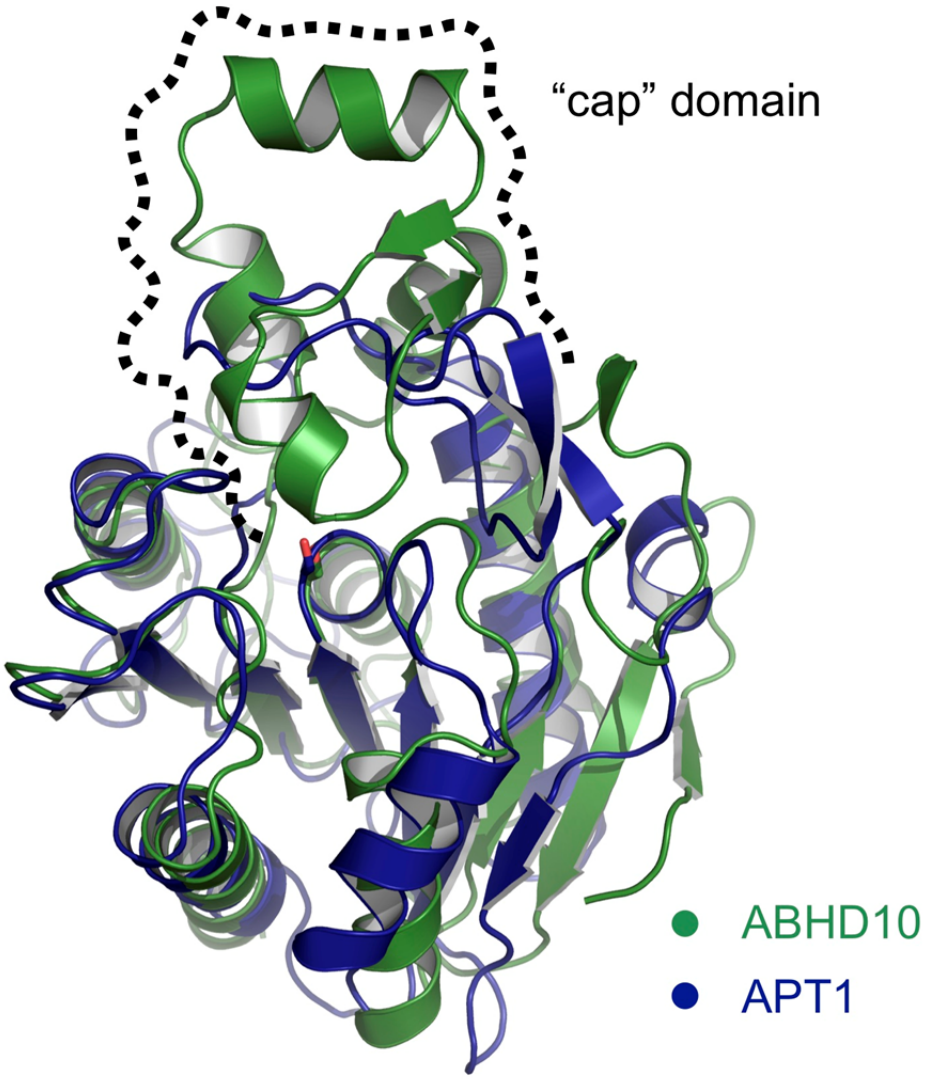

Supplementary Figure 31 | Structure alignment of mouse ABHD10 *(green)* and human APT1 *(blue,* PDB: 1FJ2*)*. The dotted black line indicates the cap domain of ABHD10, which is replaced with a loop in APT1. Both active site serines of ABHD10 and APT1 are shown in sticks.

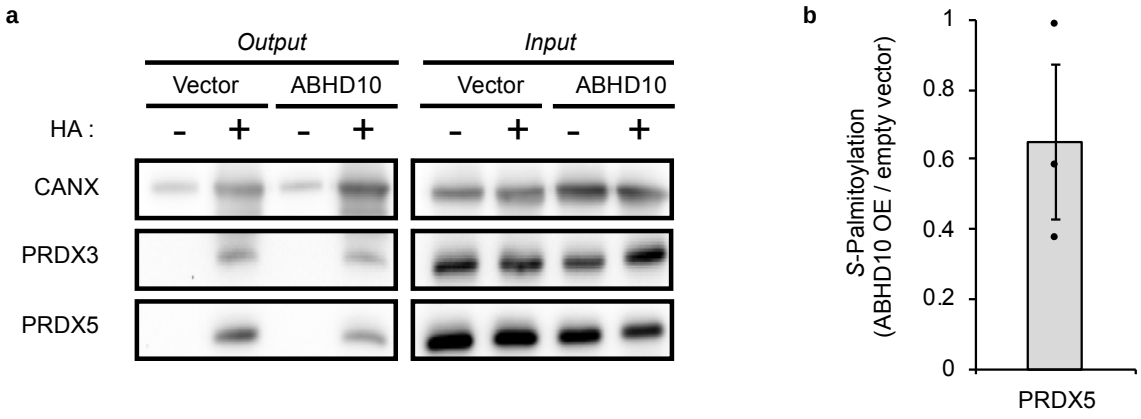

Supplementary Figure 32 | (a) ABE assay in HEK293T cells with ABHD10 overexpression compared to empty pcDNA3 vector transfected cells. PRDX5 signal decreased in ABHD10 overexpressing cells. **(b)** Quantification of relative *S*-palmitoylation levels of PRDX5 in HEK293T cells upon ABHD10 overexpression as shown in **a**. Data expressed as mean ± s.e.m (n = 3 biological replicates).

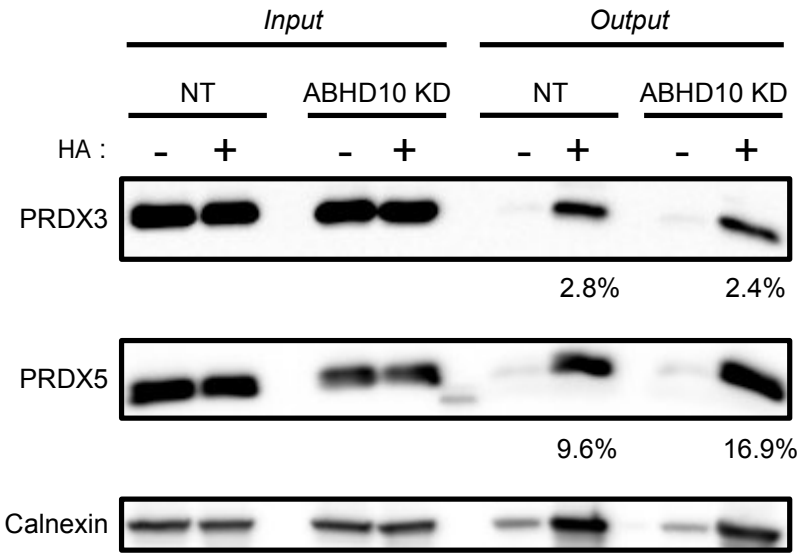

Supplementary Figure 33 | ABE assay in HeLa cells demonstrates that PRDX5 *S*-palmitoylation level increases upon ABHD10 knockdown, whereas no changes are observed for PRDX3. HeLa cells were transfected with non-targeting siRNA (NT) or ABHD10 siRNA (ABHD10 KD), grown for 36 hr, and then *S*-acylation levels were assessed by ABE. Calnexin *(CANX)* is shown as a stable *S*-palmitoylated protein control for ABE. Percentages of S-palmitoylation of PRDX3 and PRDX5 in NT and ABHD10 siRNA treated conditions are shown below respective blot. Experiment was performed once.

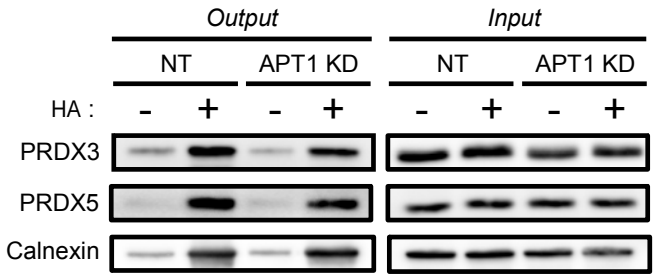

Supplementary Figure 34 | ABE assay in HEK293T cells demonstrates that APT1 knockdown does not elevate *S*-palmitoylation level of either PRDX3 or PRDX5. HEK293T cells were transfected with NT siRNA or APT1 siRNA, grown for 44 hr, and then *S*-acylation levels were assessed by ABE. Calnexin *(CANX)* is shown as a stable *S*-palmitoylated protein control for ABE. Three biological replicates were performed.

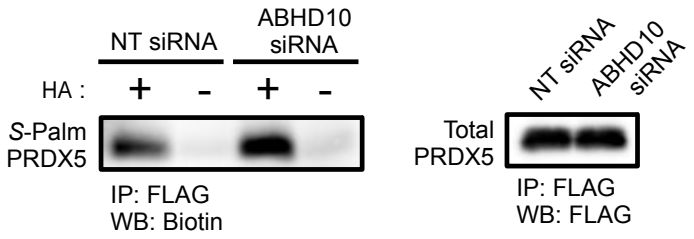

Supplementary Figure 35 | ABE assay on immunoprecipitated PRDX5-Flag expressed in HEK293T cells confirms that ABHD10 knockdown enhances *S*-palmitoylation of overexpressed PRDX5 *(left)*. HEK293T cells were transfected for 16 hr with a PRDX5-flag expression vector and then treated with either NT siRNA or ABHD10 siRNA for 24 hr, and then PRDX5-Flag was pulled down and analyzed by ABE. Two biological replicates with similar results were performed.

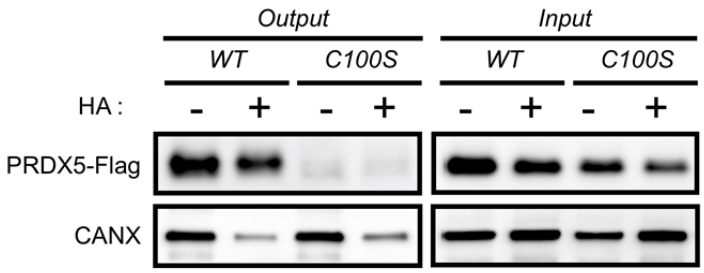

Supplementary Figure 36 | Metabolic labeling with 17-ODYA in HEK293T cells expressing PRDX5-Flag *(WT and C100S mutant)* confirms that *S*-palmitoylation occurs at catalytic site Cys^{100}. Two biological replicates with similar results were performed.

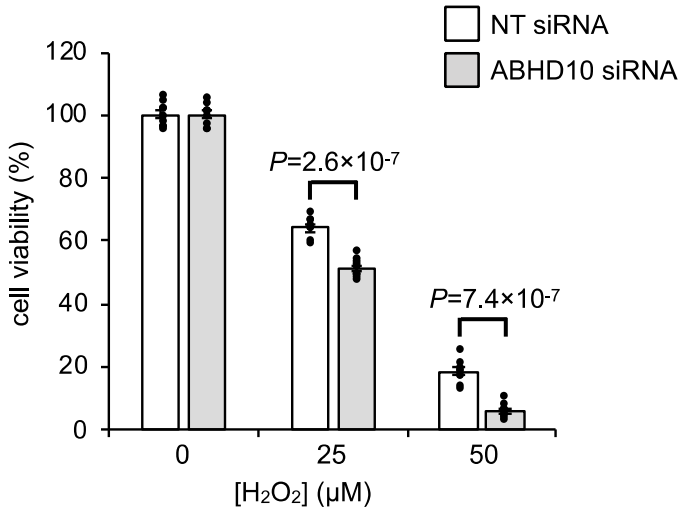

Supplementary Fig 37 | Cell viability assay in HeLa cells demonstrates that ABHD10 knockdown decreases cell survival when treated with H_2O_2. HeLa cells were transfected with either NT siRNA or ABHD10 siRNA and grown for 48 hr, challenged with varying concentrations of H_2O_2 for 36 hr, and then analyzed for viability by the MTS assay. Statistical analyses performed with a two-tailed Student's *t*-test with unequal variance (n = 9 biological replicates). Data expressed as mean ± s.e.m. and each group of cells with various concentrations of H_2O_2 is normalized to respective cells treated with H_2O.

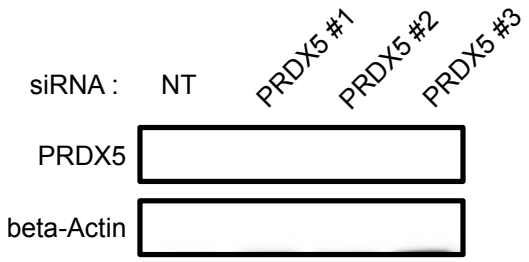

Supplementary Figure 38 | Knockdown efficiency of PRDX5 analyzed by western blots. 3 siRNAs were screened to find out best siRNA for further studies.We chose #3 SiRNA to perform further experiments. Beta-Actin was used as loading control. *NT:* Non-targeting siRNA.

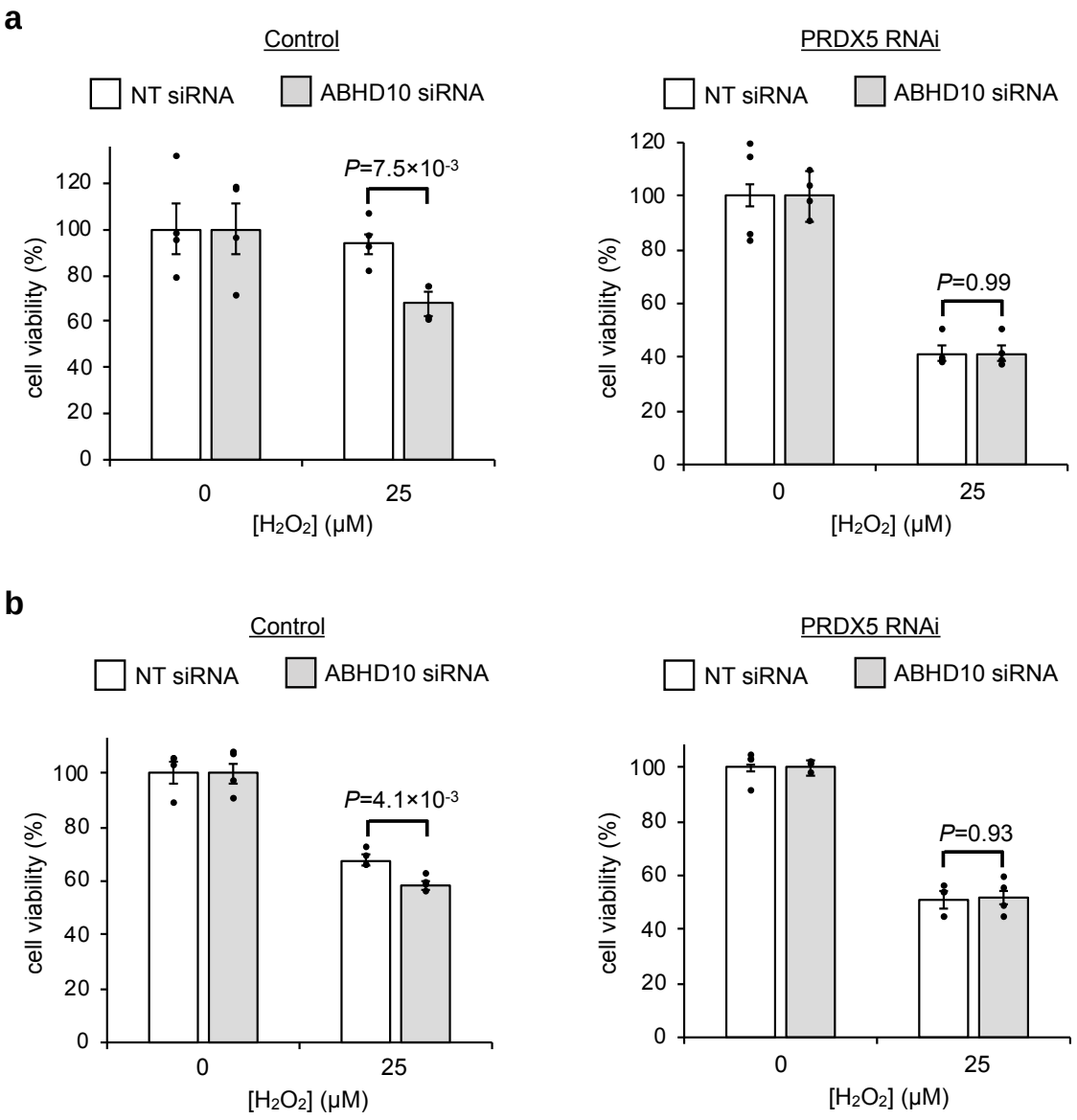

Supplementary Fig 39 | Cell viability assays in **(a)** HEK293T cells and **(b)** HeLa cells demonstrate the effect of ABHD10 knockdown induced cell death *(left panel)* when treated with 25 μM H_2O_2 is abrogated when PRDX5 is knockdown *(right panel).* HEK293T and HeLa cells were transfected with either NT siRNA, PRDX5 siRNA, ABHD10 siRNA or cotransfection of ABHD10 siRNA and PRDX5 siRNA for 24h before replating to 96 wells plate. After 24h, cells were challenged with 25 μM of H_2O_2 for 36 hr and then analyzed for viability by the MTS assay. Statistical analyses performed with a two-tailed Student's *t*-test with unequal variance (n = 4 biological replicates). Data expressed as mean ± s.e.m. and cells treated with 25 μM H_2O_2 are normalized to respective cells treated with NT or ABHD10 siRNA and H_2O.

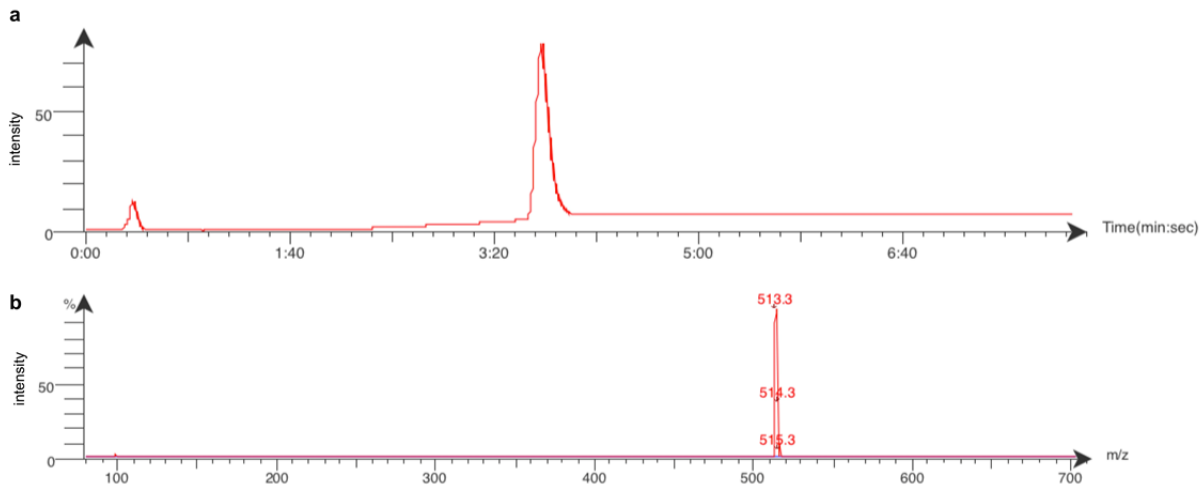

Supplementary Figure 40 | Purity of mitoFP analyzed by LCMS. (**a**) UV signal at 254 nm. (**b**) ESI (+) shows m/z at 513.3 for mitoFP. Experiment done once.

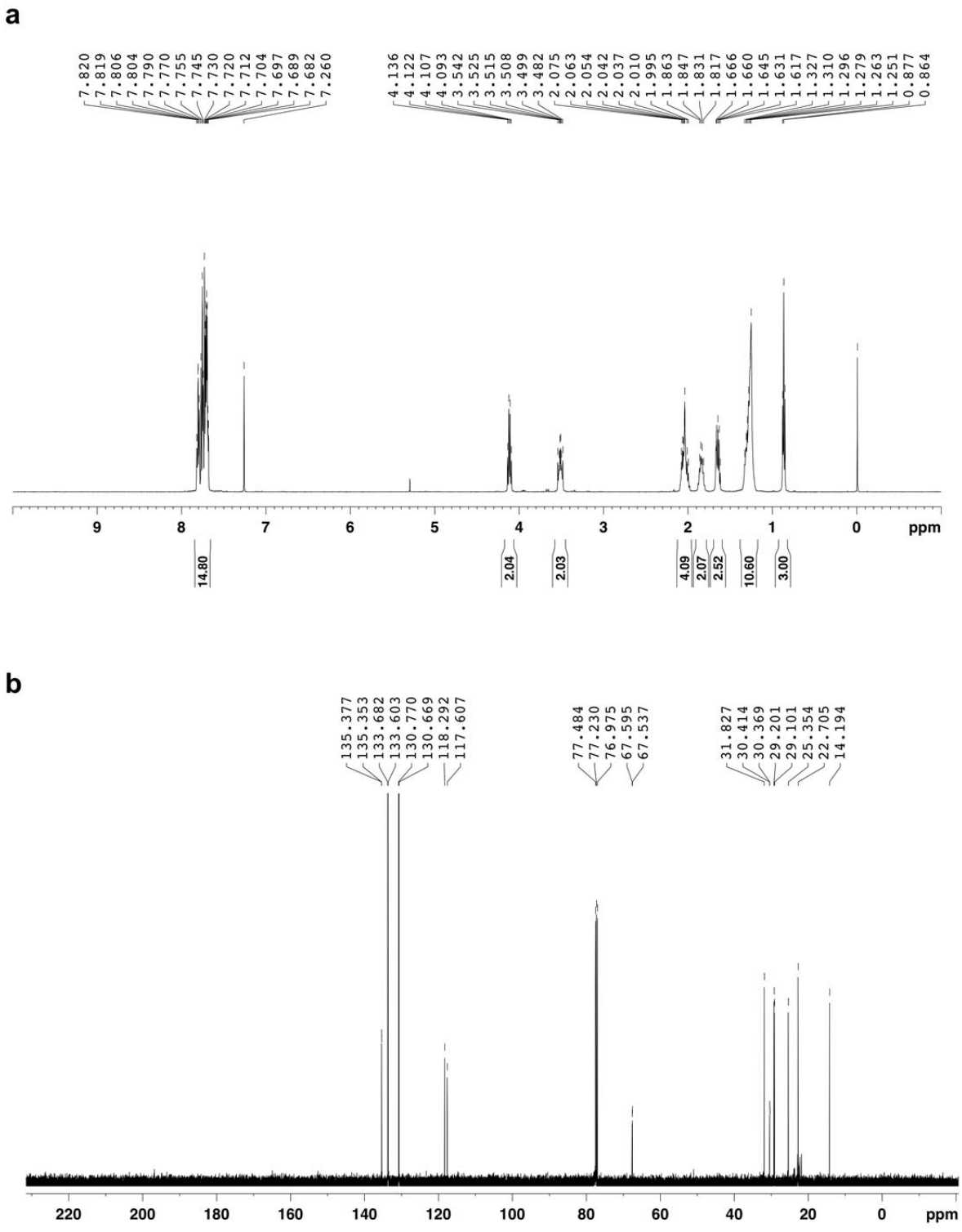

Supplementary Figure 41 | NMR analysis of mitoFP. ^{1}H NMR (**a**) and ^{13}C NMR (**b**) in $CDCl_3$.

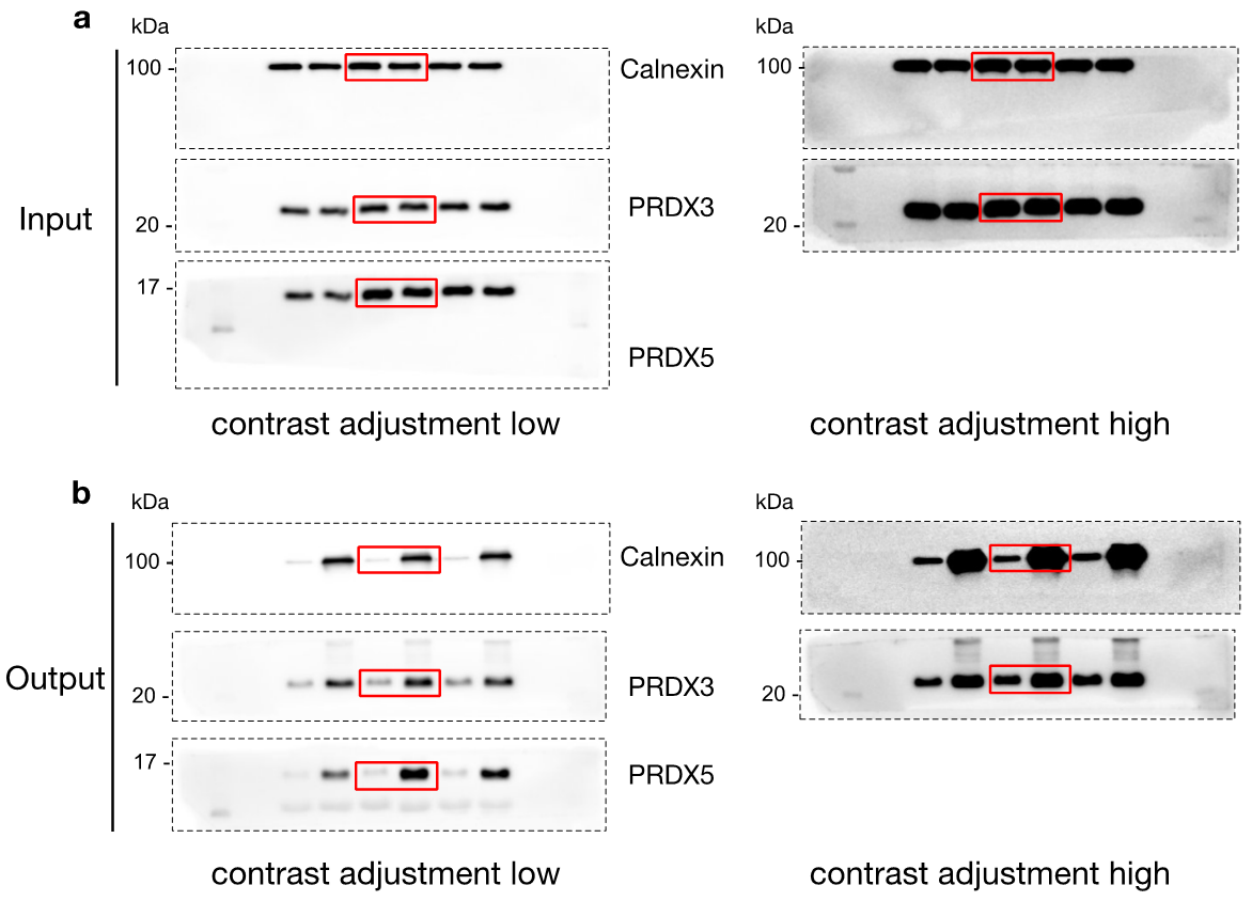

Supplementary Figure 42 | Uncropped Western blots related to Figure 1c.

.

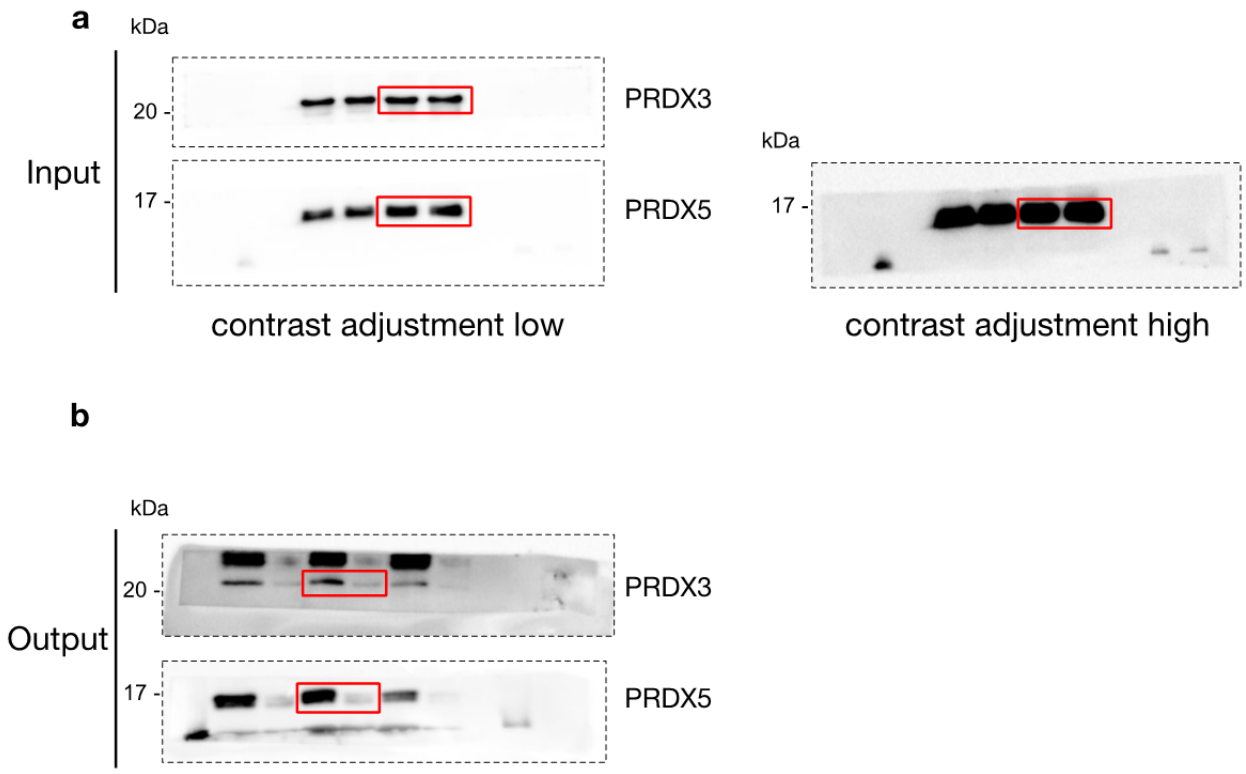

Supplementary Figure 43 | Uncropped Western blots related to Figure 1d.

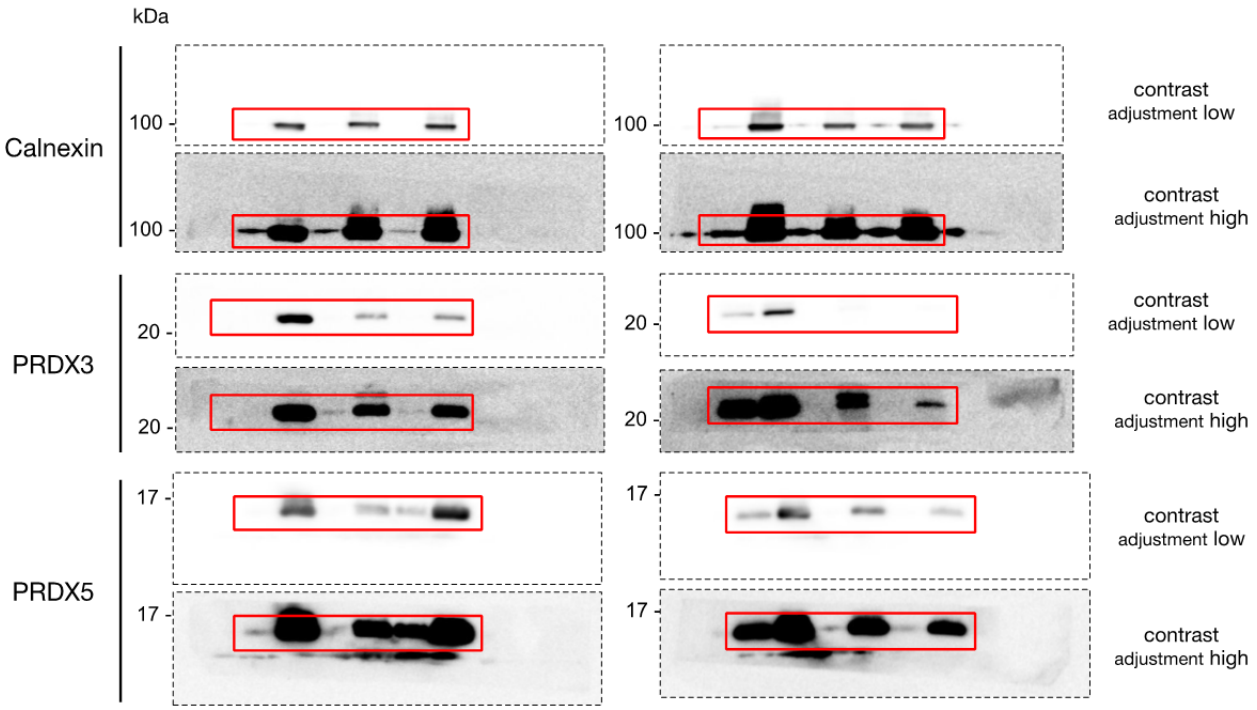

Supplementary Figure 44 | Uncropped Western blots related to Figure 1e.

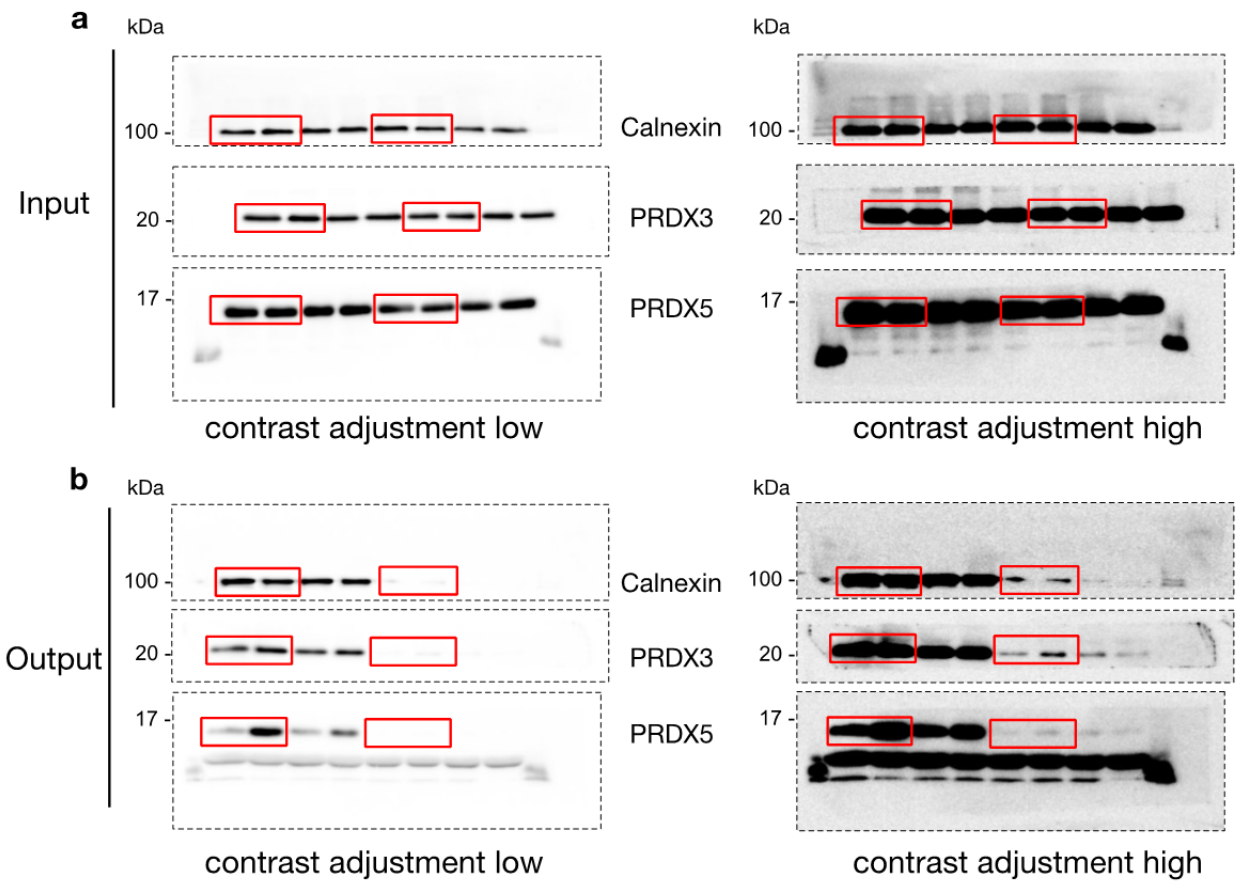

Supplementary Figure 45 | Uncropped Western blots related to Figure 1f.

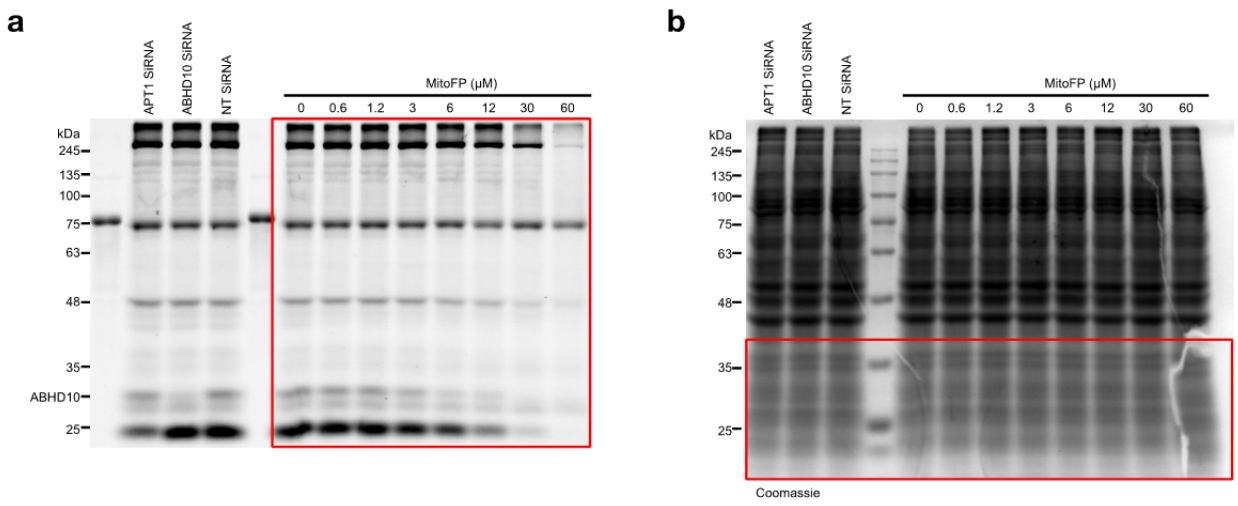

Supplementary Figure 46 | Uncropped Western blots related to Figure 3c.

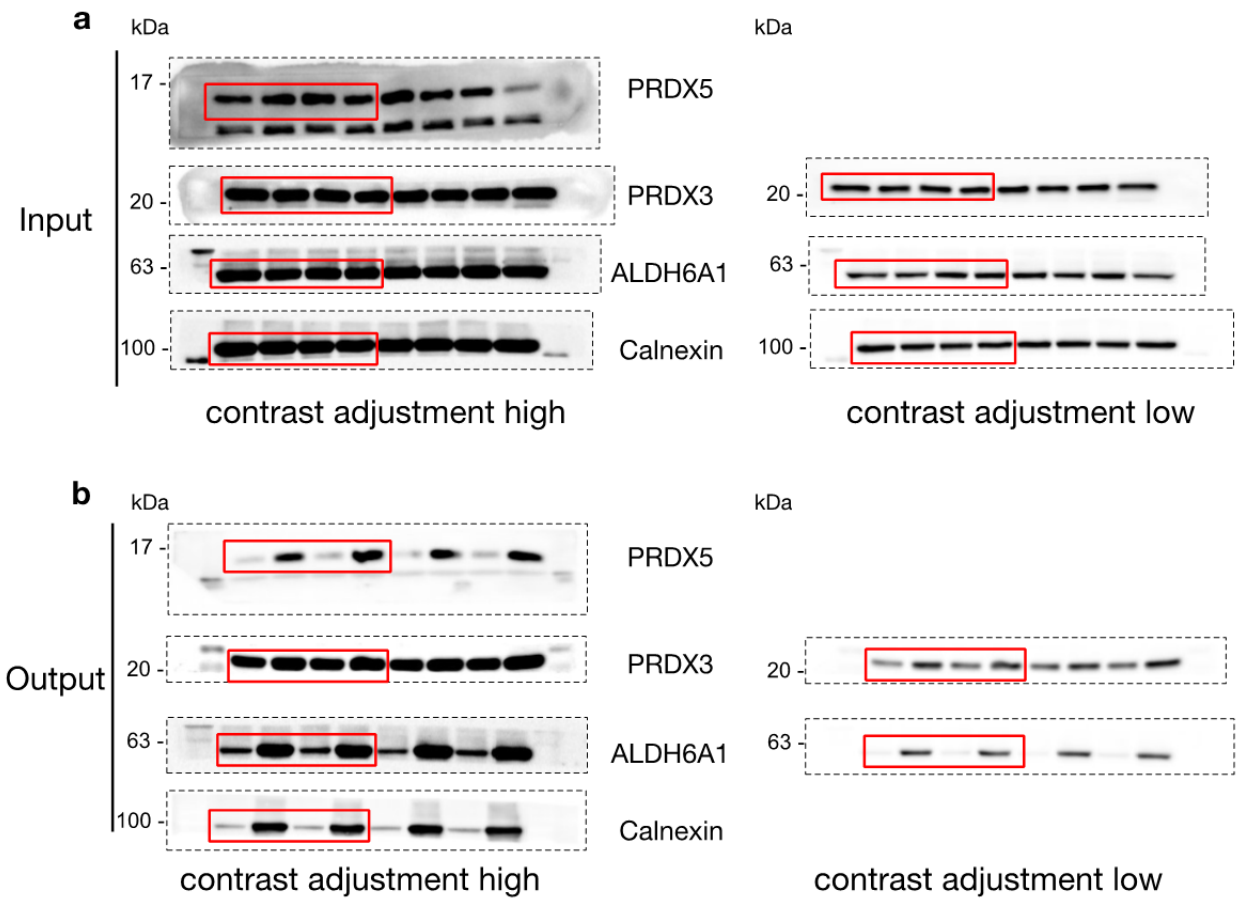

Supplementary Figure 47 | Uncropped Western blots related to Figure 5a.

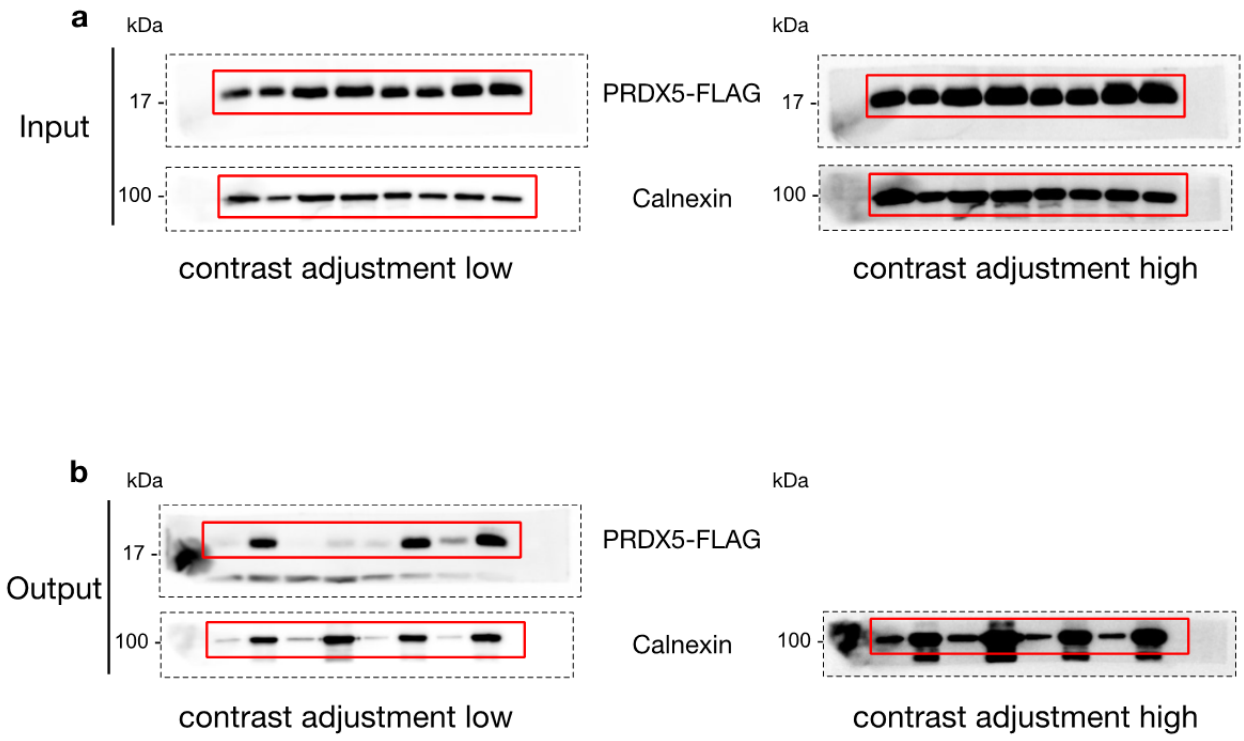

Supplementary Figure 48 | Uncropped Western blots related to Figure 5d.

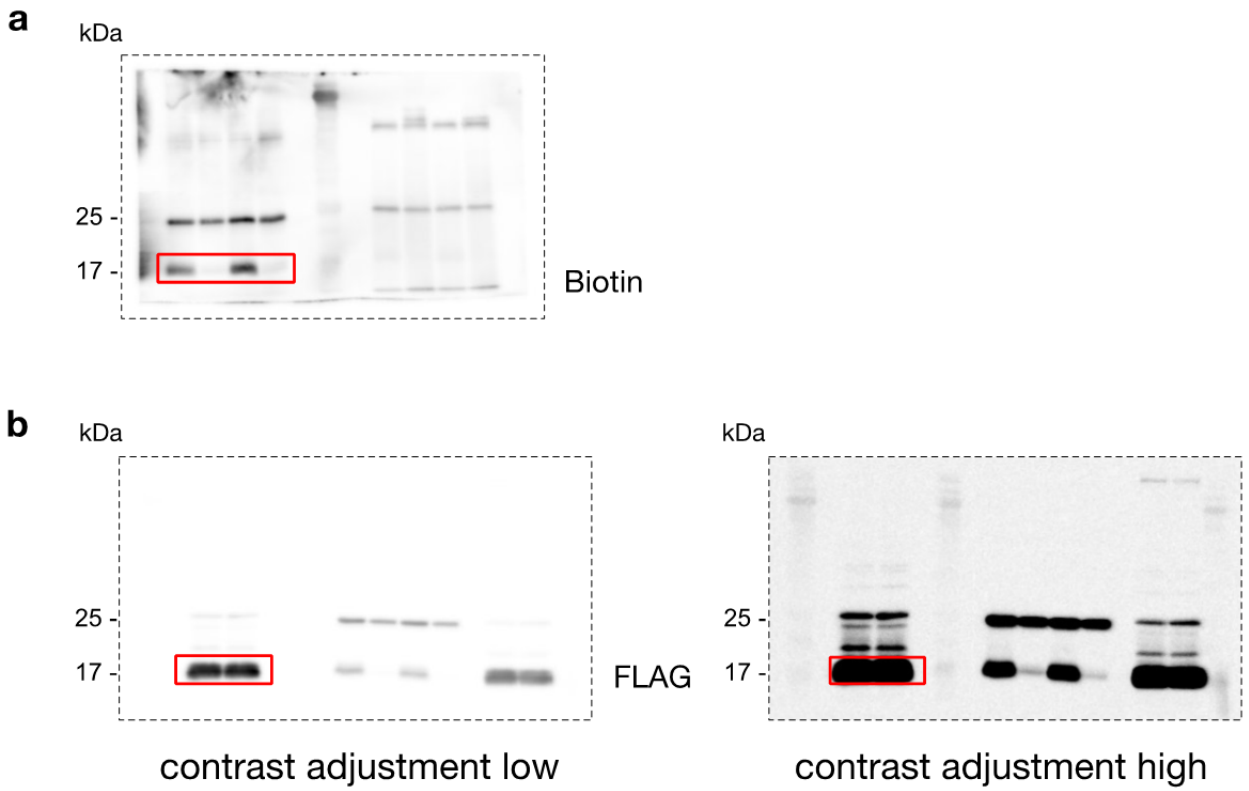

Supplementary Figure 49 | Uncropped Western blots related to Supplementary Figure 35.

References

1. Kathayat, R.S., Elvira, P.D. & Dickinson, B.C. A fluorescent probe for cysteine depalmitoylation reveals dynamic APT signaling. *Nat Chem Biol* **13**, 150-152 (2017).
2. Qiu, T., Kathayat, R.S., Cao, Y., Beck, M.W. & Dickinson, B.C. A Fluorescent Probe with Improved Water Solubility Permits the Analysis of Protein S-Depalmitoylation Activity in Live Cells. *Biochemistry* **57**, 221-225 (2018).
3. Kathayat, R.S. *et al.* Active and dynamic mitochondrial S-depalmitoylation revealed by targeted fluorescent probes. *Nat Commun* **9**, 334 (2018).